# Lectures on Theoretical Cosmology

Raphael Flauger
UC San Diego

TRISEP, Perimeter Institute, July 16 2018

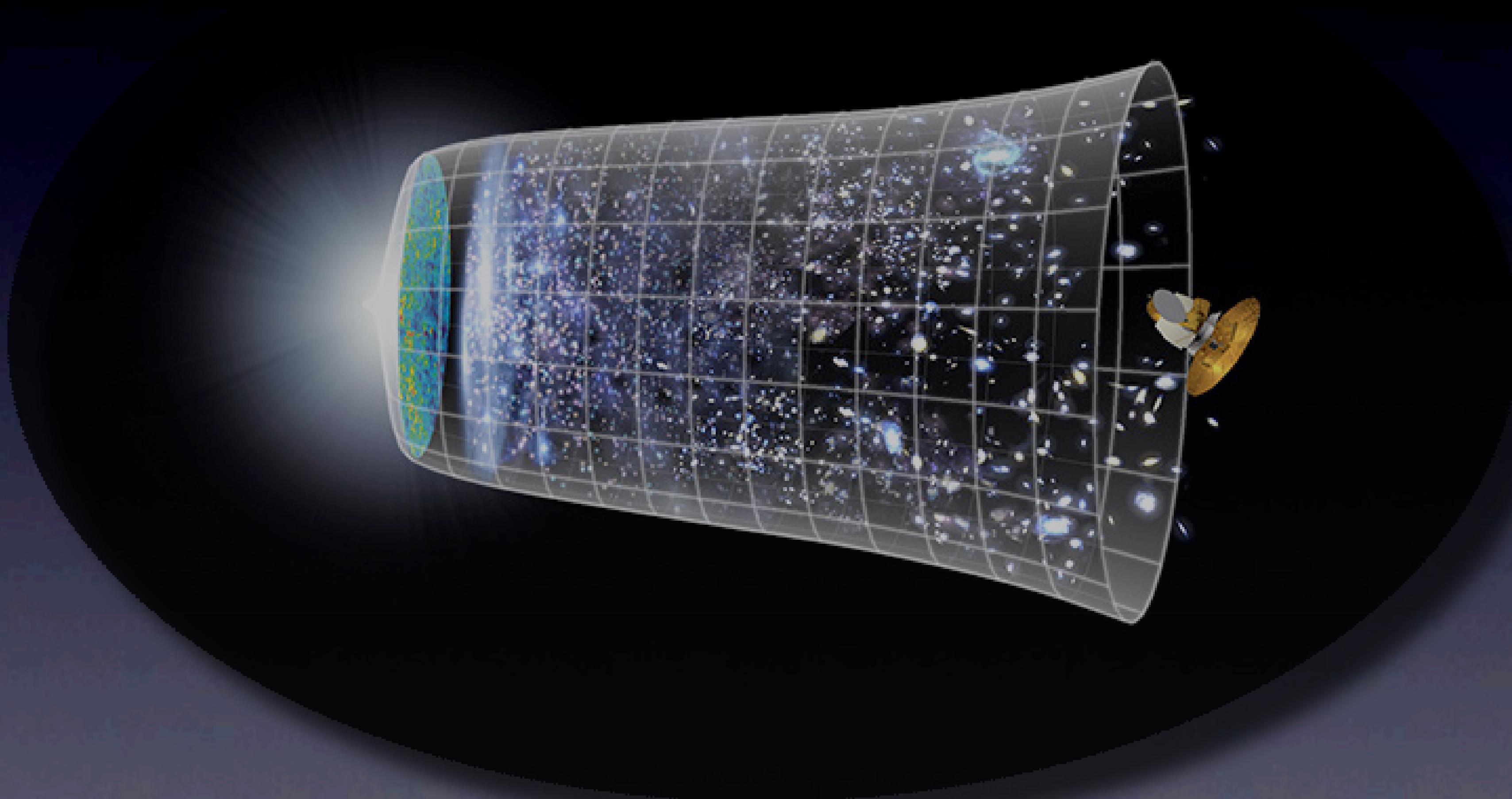

(NASA/WMAP Science Team)

# General Relativity - Part I

# Geometry of Spacetime

Zur allgemeinen Relativitätstheorie.

Von A. Einstein.

(Einstein 1915)

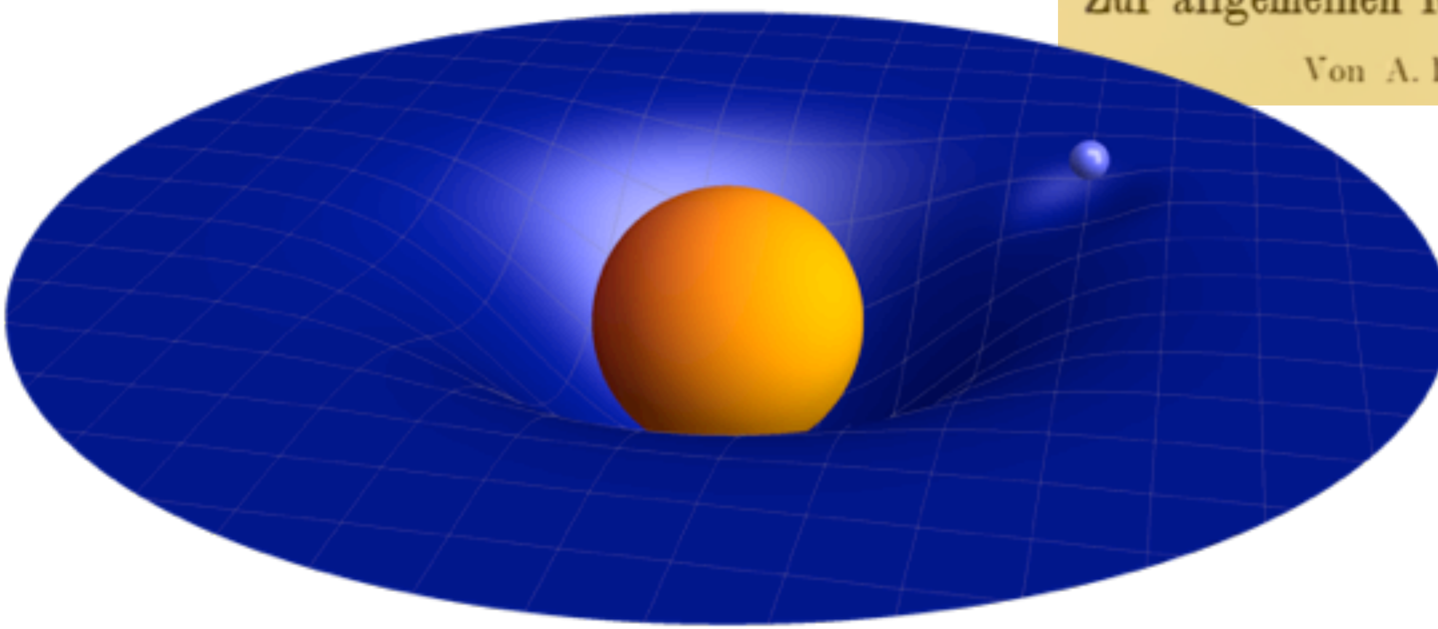

# Geometry of Spacetime

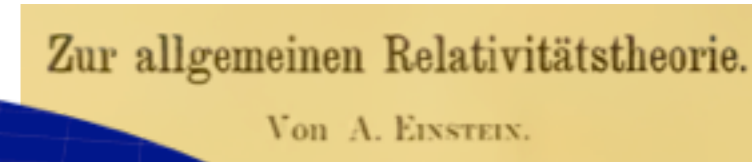
Zur allgemeinen Relativitätstheorie.

Von A. Einstein.

(Einstein 1915)

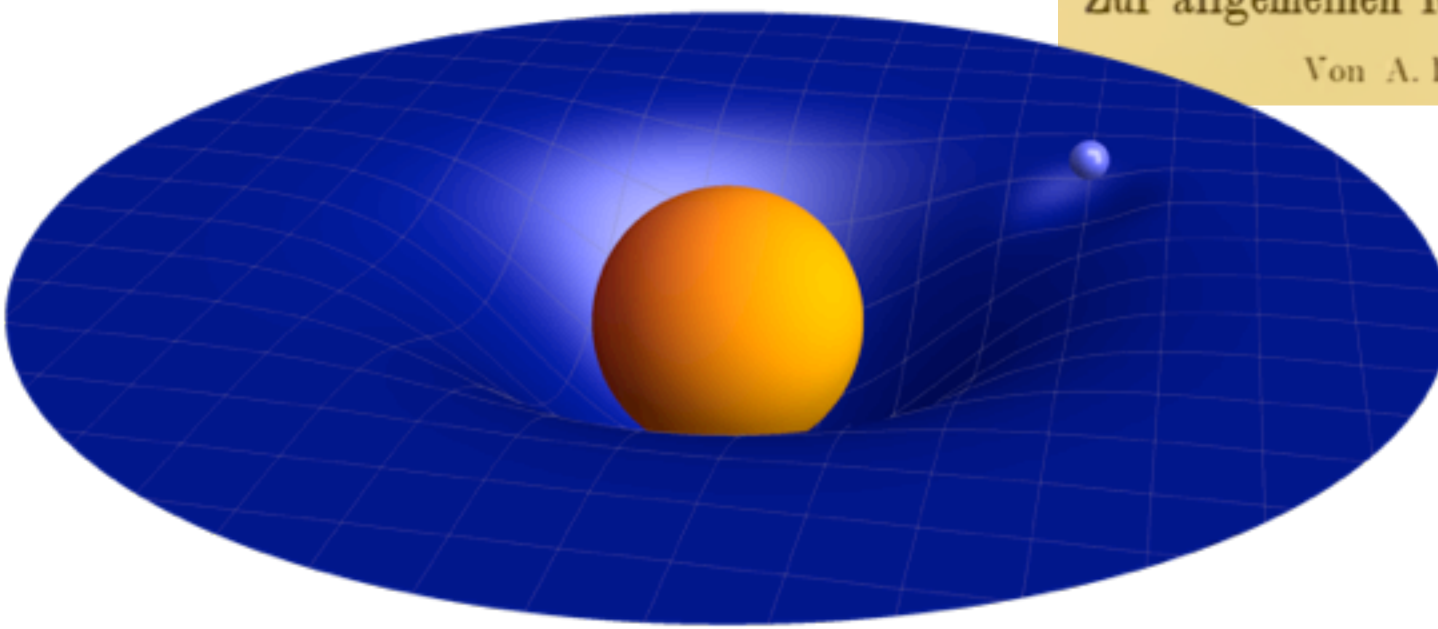

- Gravitational attraction arises because spacetime is curved.
- The geometry of spacetime is determined by the matter distribution.

# Geometry of Spacetime

The geometry of space is encoded by the line element

$$ds^2 = \sum_{ij} g_{ij} dx^i dx^j \equiv g_{ij} dx^i dx^j$$

Ueber

die Hypothesen, welche der Geometrie zu Grunde liegen.

Von

B. Riemann.

**(Riemann 1854)**

# Geometry of Spacetime

The geometry of space is encoded by the line element

Ueber

die Hypothesen, welche der Geometrie zu Grunde liegen.

Von

B. Riemann.

**(Riemann 1854)**

$$ds^2 = \sum_{ij} g_{ij} dx^i dx^j \equiv g_{ij} dx^i dx^j$$

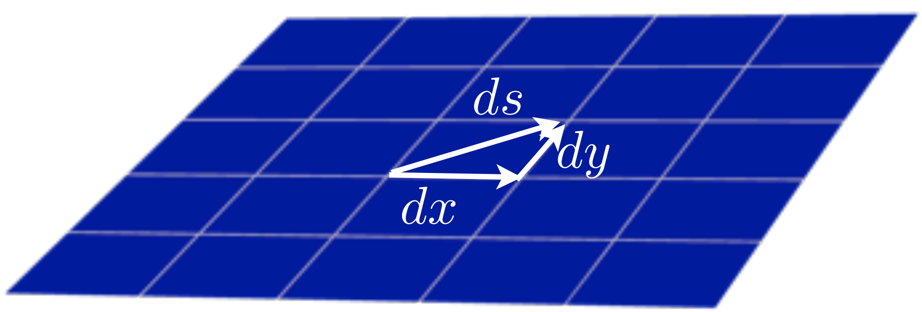


$$ds^2 = dx^2 + dy^2$$

# Geometry of Spacetime

The geometry of space is encoded by the line element

$$ds^2 = \sum_{ij} g_{ij}\, dx^i dx^j \equiv g_{ij}\, dx^i dx^j$$

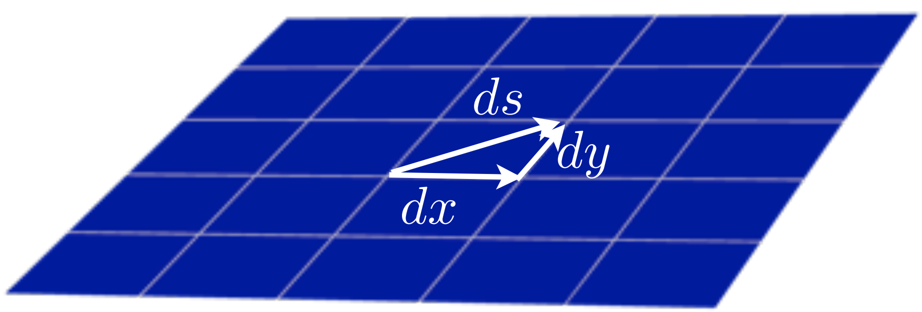


$$ds^2 = dx^2 + dy^2$$

Ueber
die Hypothesen, welche der Geometrie zu Grunde liegen.
Von
B. Riemann.

**(Riemann 1854)**

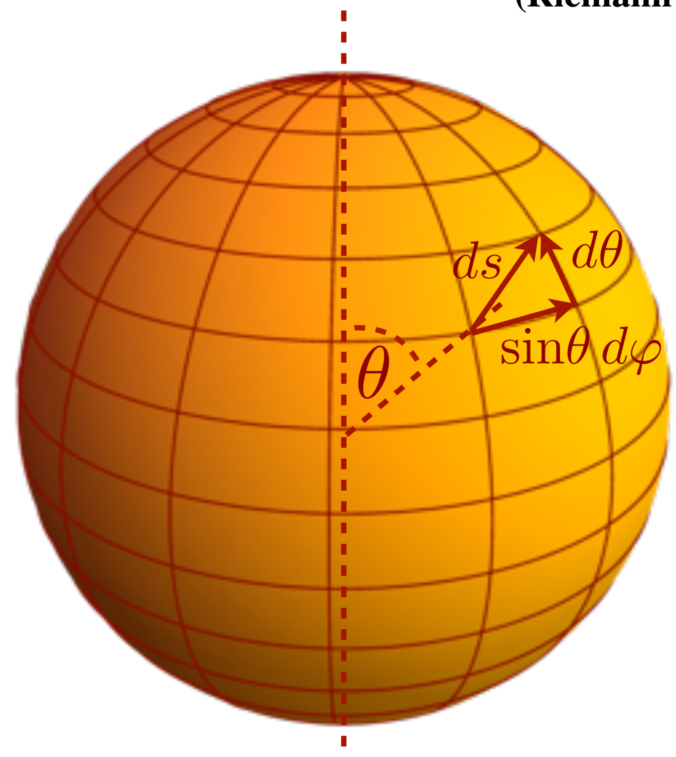


$$ds^2 = d\theta^2 + \sin^2\theta\, d\varphi^2$$

# Geometry of Spacetime

1. *Die Grundlage*
*der allgemeinen Relativitätstheorie;*
*von A. Einstein.*

**(Einstein 1916)**

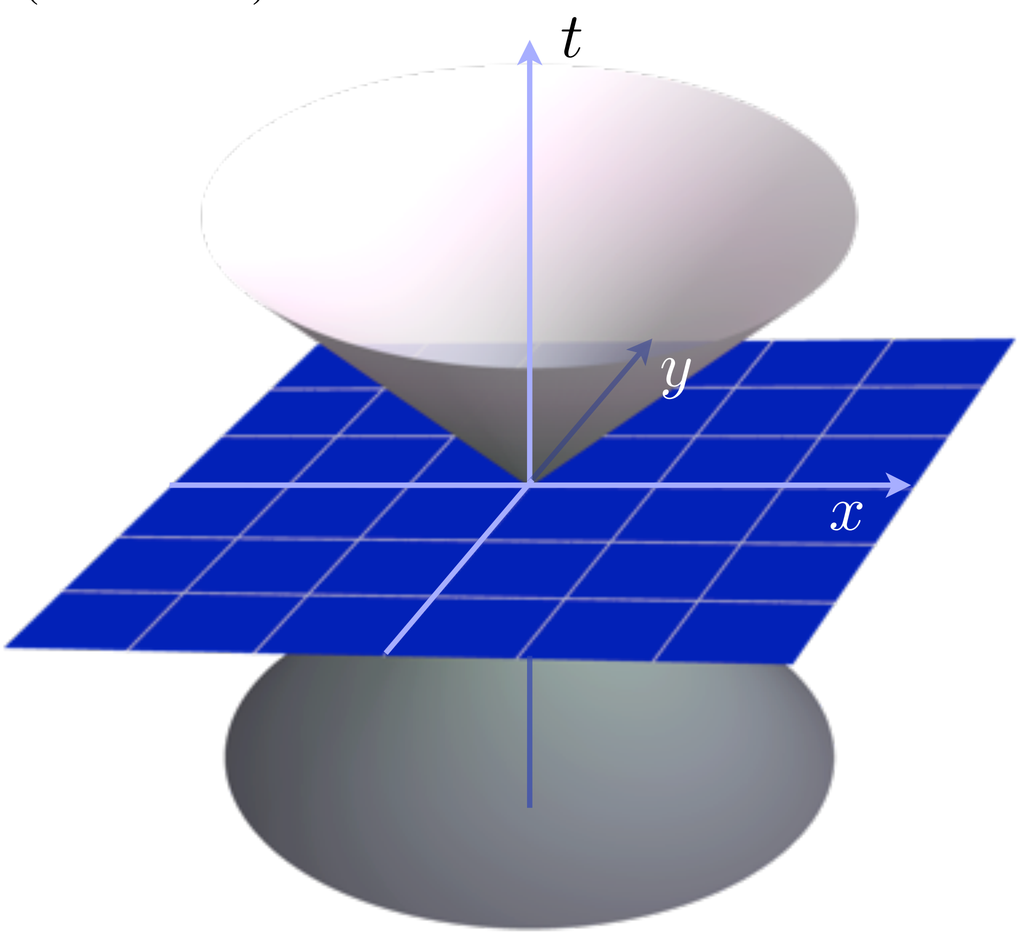


The geometry of spacetime is encoded by the line element

$$ds^2 = g_{\mu\nu} dx_\mu dx_\nu$$

$$ds^2 = -dt^2 + d\vec{x}^2$$

# Geometry of Spacetime

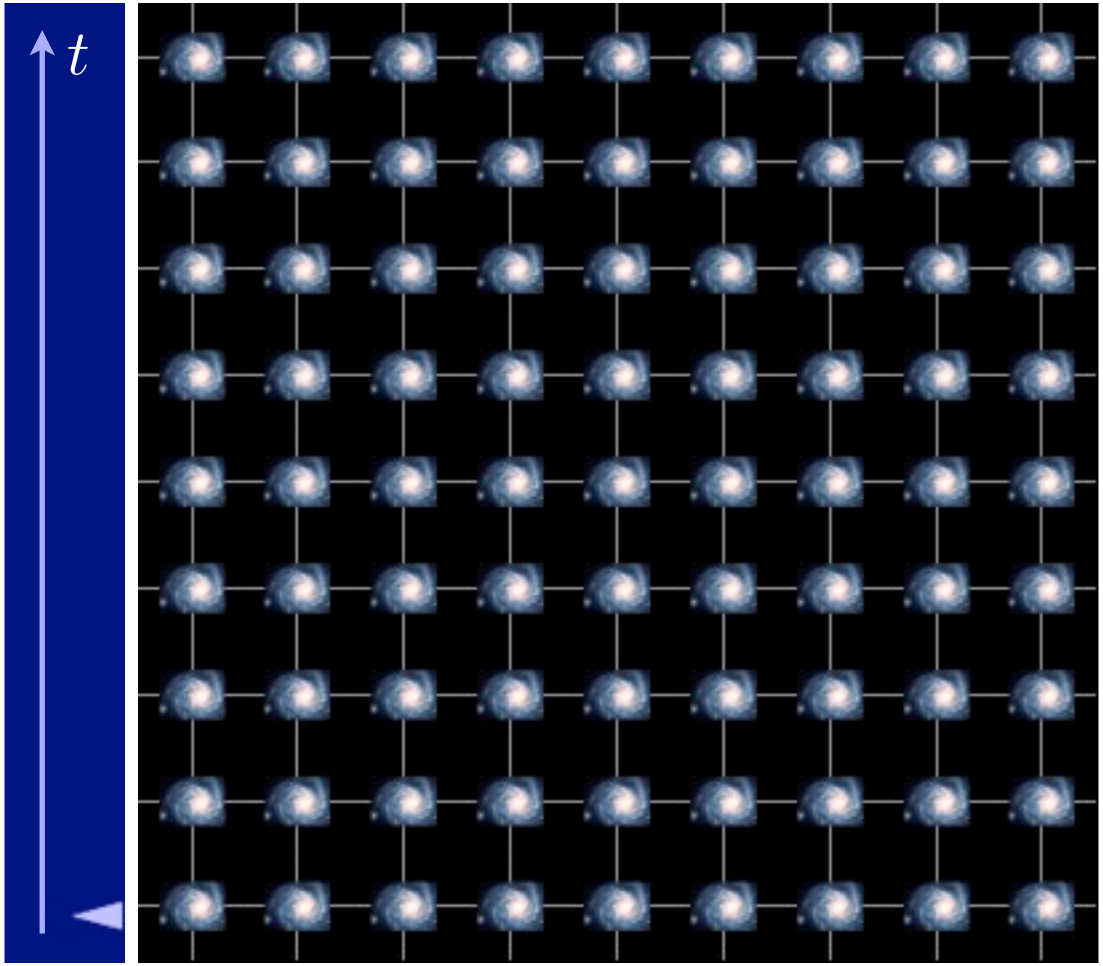


At $t = t_1$: $ds^2 = a_1^2 d\vec{x}^2$

# Geometry of Spacetime

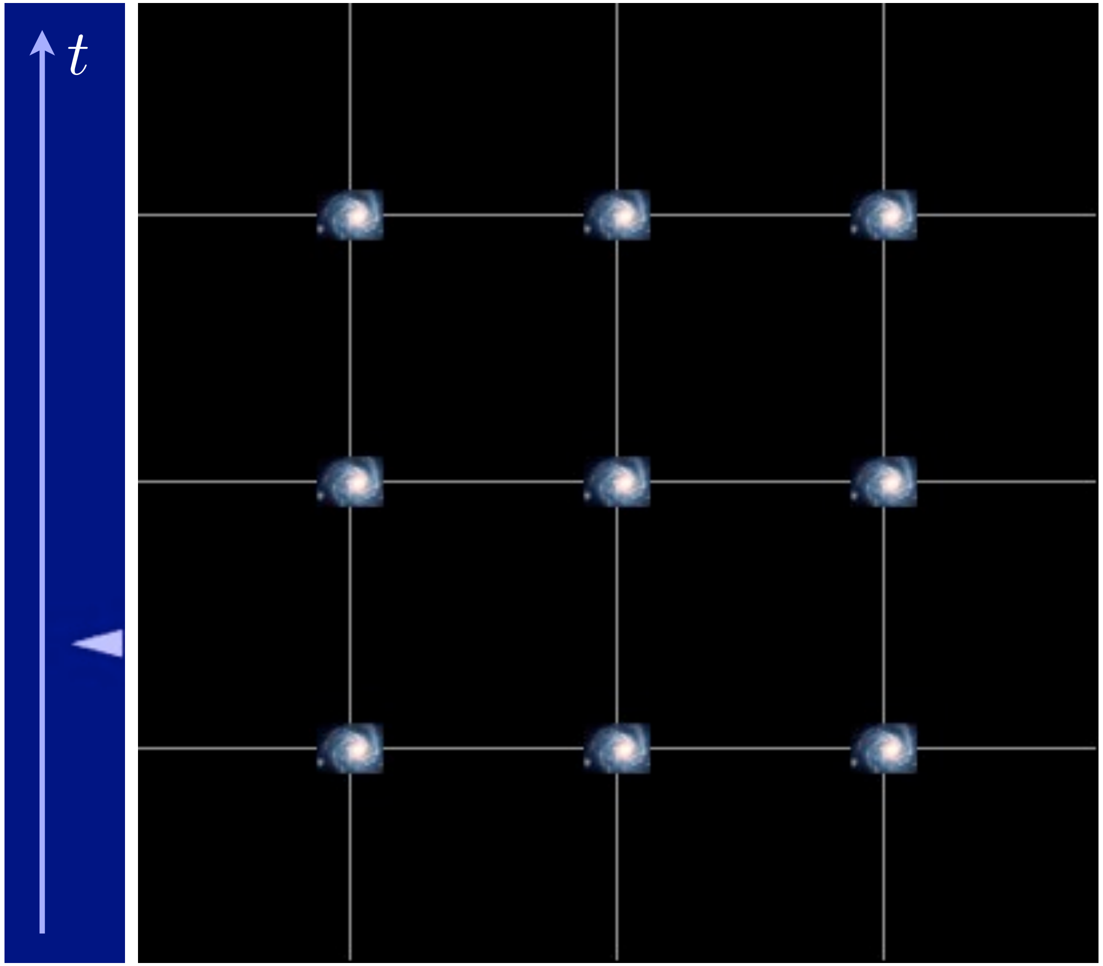


At $t = t_2$: $ds^2 = a_2^2 d\vec{x}^2$

# Geometry of Spacetime

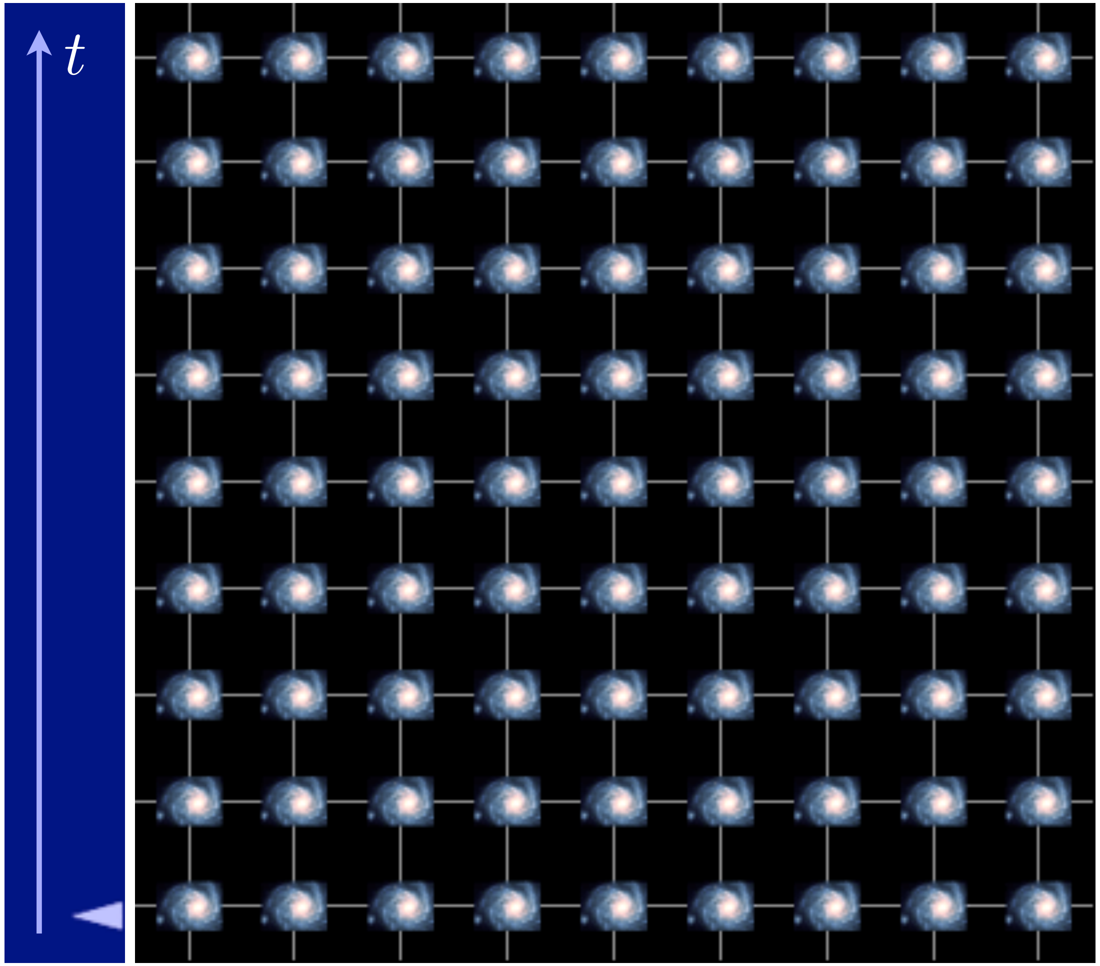


$$ds^2 = -dt^2 + a^2(t)d\vec{x}^2$$

# Geometry of Spacetime

More generally

$$ds^2 = -dt^2 + a^2(t)\left[d\vec{x}^2 + K\frac{(\vec{x}\cdot d\vec{x})^2}{1-K\vec{x}^2}\right]$$

$$K = \begin{cases} 1 & \text{closed} \\ -1 & \text{open} \\ 0 & \text{flat} \end{cases}$$

Currently all data is consistent with a flat universe

$$ds^2 = -dt^2 + a^2(t)d\vec{x}^2$$

# Geometry of Spacetime

The geometry of our universe is thus encoded by the "scale factor" $a(t)$.

# Geometry of Spacetime

The geometry of our universe is thus encoded by the "scale factor" $a(t)$.

In a spatially flat universe, physical quantities are independent of its normalization:

$$H(t) \equiv \frac{\dot{a}(t)}{a(t)}$$

expansion or Hubble rate

$$\frac{a(t)}{a(t_0)} = \frac{1}{1+z}$$

redshift

# Particles in the FLRW Universe

The motion of "particles" is governed by the action

$$S = -m \int d\tau \sqrt{-g_{\mu\nu} \dot{x}^\mu \dot{x}^\nu}$$

This leads to the equations of motion

$$\frac{d^2 x^\mu}{d\tau} + \Gamma^\mu_{\nu\rho} \frac{dx^\nu}{d\tau} \frac{dx^\rho}{d\tau} = 0 \qquad \text{(geodesic equation)}$$

with

$$\Gamma^\mu_{\nu\rho} = \frac{1}{2} g^{\mu\sigma} \left( \frac{\partial g_{\sigma\nu}}{\partial x^\rho} + \frac{\partial g_{\sigma\rho}}{\partial x^\nu} - \frac{\partial g_{\nu\rho}}{\partial x^\sigma} \right)$$

or in the flat FLRW universe

$$\ddot{x}^0 + a\dot{a}\delta_{ij}\dot{x}^i \dot{x}^j = 0\,,$$

$$\ddot{x}^i + 2H\dot{x}^i \dot{x}^0 = 0\,.$$

# Particles in the FLRW Universe

Using

$$\frac{d}{d\tau} = \frac{dx^0}{d\tau}\frac{d}{dt}$$

the second equation becomes

$$\frac{d}{dt}\frac{dx^i}{d\tau} + 2H\frac{dx^i}{d\tau} = 0$$

so that

$$\frac{dx^i}{d\tau} \propto \frac{1}{a(t)^2}$$

# Particles in the FLRW Universe

The momentum of a particle is as usual

$$p_\mu = \frac{\partial L}{\partial \dot{x}^\mu} = \frac{m g_{\mu\nu} \dot{x}^\nu}{\sqrt{-g_{\rho\sigma} \dot{x}^\rho \dot{x}^\sigma}}$$

or choosing the affine parameter such that $1 = -g_{\rho\sigma} \dot{x}^\rho \dot{x}^\sigma$

$$p_\mu = m g_{\mu\nu} \dot{x}^\nu$$

The magnitude of the 3-momentum of a particle then behaves as

$$p = m \sqrt{g_{ij} \frac{dx^i}{d\tau} \frac{dx^j}{d\tau}} \propto \frac{1}{a(t)}$$

# Particles in the FLRW Universe

The momentum of a particle emitted at time $t$ with momentum $p$ is redshifted to

$$p_0 = p\frac{a(t)}{a(t_0)} = \frac{p}{1+z} \quad \text{today.}$$

This remains true for massless particles.

Since $p = h\nu$, their frequencies then redshift as

$$\nu_0 = \nu\frac{a(t)}{a(t_0)} = \frac{\nu}{1+z}$$

# The expanding universe

Turning to the expansion rate, note that for nearby events, we can expand the scale factor

$$a(t) = a(t_0) + \dot{a}(t_0)(t - t_0) + \ldots$$

For $z \ll 1$, this is

$$z = H_0(t_0 - t)$$

or

$$z = H_0 d$$

In an expanding universe, we should predominantly see galaxies with $z > 0$.

# The expanding universe

V.M. Slipher

# The expanding universe

SPECTROGRAPHIC OBSERVATIONS OF NEBULAE.

By V. M. Slipher.

1913

During the last two years the spectrographic work at Flagstaff has been devoted largely to nebulae. While the observations were chiefly concerned with the spiral nebulae they also include planetary and extended nebulae and globular star clusters.

| | | | |
|---|---|---|---|
| N.G.C. | 221 | Velocity — 300 km | These nebulae are on the south side of the Milky Way. |
| | 224 † | — 300 | |
| | 598 | — | |
| | 1023 | + 200 roughly | |
| | 1068 | + 1100 | |
| | 7331 | + 300 roughly | |
| | 3031 | + small | These are on the north side of the Milky Way |
| | 3115 | + 400 roughly | |
| | 3627 | + 500 | |
| | 4565 | + 1000 | |
| | 4594 | + 1100 | |
| | 4736 | + 200 roughly | |
| | 4826 | + small | |
| | 5194 | ± small | |
| | 5866 | + 600 | |

As far as the data go, the average velocity is 400 km.

# The expanding universe

To measure more than the sign of the expansion rate requires distance measurements

- Parallax

- Luminosity distance

$$\ell = \frac{L}{4\pi d^2}$$

Euclidean space

$$\ell = \frac{L}{4\pi d_L^2}$$

FLRW universe

$$d_L = a_0 r(1+z)$$

- Angular diameter distance $s = \theta d_A = \dfrac{\theta a_0 r}{1+z}$

# The expanding universe

To use them we need

Standard candles

- Certain variable stars
- Type Ia Supernovae

Standard rulers

- Baryon acoustic oscillations

Standard sirens

- Gravitational wave events with electromagnetic counterpart

# The expanding universe

H.S. Leavitt

# The expanding universe

1777 VARIABLES IN THE MAGELLANIC CLOUDS.

By Henrietta S. Leavitt. 1908

PERIODS OF VARIABLES IN THE SMALL MAGELLANIC CLOUD.

| Harvard No. | Max. | Min. | Range. | Epoch. | Period. | Min. to Max. | Average Dev. | Earliest Observation. | No. Periods. | No. Plates. |
|---|---|---|---|---|---|---|---|---|---|---|
| | | | | | d. | d. | | | | |
| 818 | 13.6 | 14.7 | 1.1 | 4.0 | 10.336 | 1.7 | .12 | 1890 | 566 | 44 |
| 821 | 11.2 | 12.1 | 0.9 | 97. | 127. | 49. | .06 | 1890 | 45 | 89 |
| 823 | 12.2 | 14.1 | 1.9 | 2.9 | 31.94 | 3. | .13 | 1890 | 184 | 56 |
| 824 | 11.4 | 12.8 | 1.4 | 4. | 65.8 | 7. | .12 | 1889 | 94 | 83 |
| 827 | 13.4 | 14.3 | 0.9 | 11.6 | 13.47 | 6. | .11 | 1890 | 448 | 60 |
| 842 | 14.6 | 16.1 | 1.5 | 2.61 | 4.2897 | 0.6 | .06 | 1896 | 843 | 26 |
| 1374 | 13.9 | 15.2 | 1.3 | 6.0 | 8.397 | 2. | .10 | 1893 | 574 | 42 |
| 1400 | 14.1 | 14.8 | 0.7 | 4.0 | 6.650 | 1. | .11 | 1893 | 724 | 42 |
| 1425 | 14.3 | 15.3 | 1.0 | 2.8 | 4.547 | 0.8 | .09 | 1893 | 1042 | 33 |
| 1436 | 14.8 | 16.4 | 1.6 | 0.02 | 1.6637 | 0.3 | .10 | 1893 | 2859 | 22 |
| 1446 | 14.8 | 16.4 | 1.6 | 1.38 | 1.7620 | 0.3 | .09 | 1896 | 2052 | 21 |
| 1505 | 14.8 | 16.1 | 1.3 | 0.02 | 1.25336 | 0.2 | .10 | 1896 | 2335 | 25 |
| 1506 | 15.1 | 16.3 | 1.2 | 1.08 | 1.87502 | 0.3 | .09 | 1896 | 1560 | 23 |
| 1646 | 14.4 | 15.4 | 1.0 | 4.30 | 5.311 | 0.7 | .06 | 1896 | 681 | 24 |
| 1649 | 14.3 | 15.2 | 0.9 | 5.05 | 5.323 | 0.7 | .10 | 1893 | 894 | 32 |
| 1742 | 14.3 | 15.5 | 1.2 | 0.95 | 4.9866 | 0.7 | .07 | 1893 | 954 | 28 |

It is worthy of notice that in Table VI the brighter variables have the longer periods.

# The expanding universe

HARVARD COLLEGE OBSERVATORY.

1912

CIRCULAR 173.

PERIODS OF 25 VARIABLE STARS IN THE SMALL MAGELLANIC CLOUD.

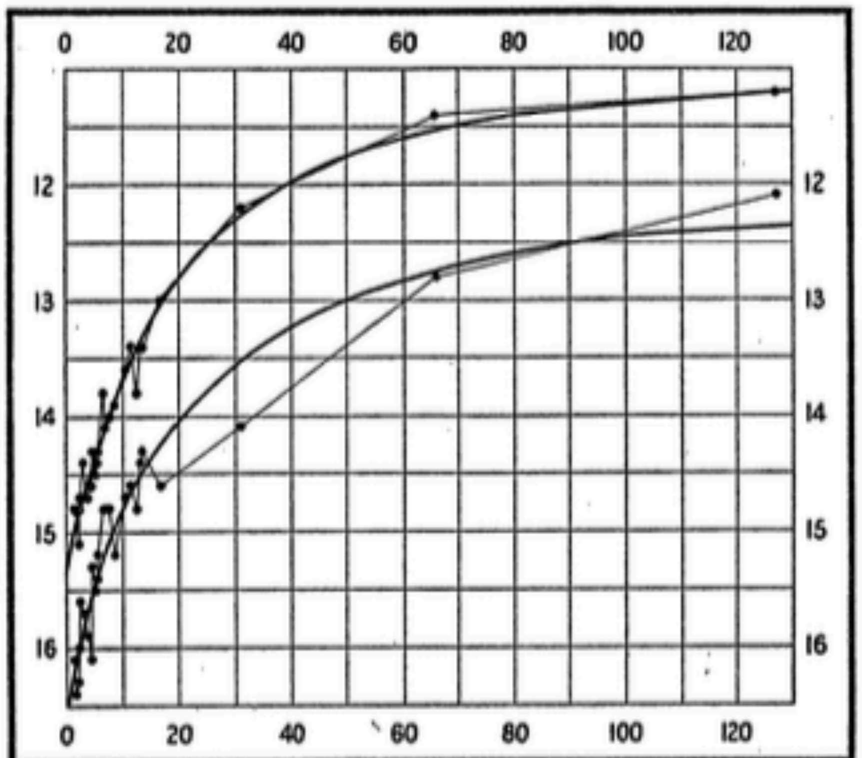


FIG. 1.

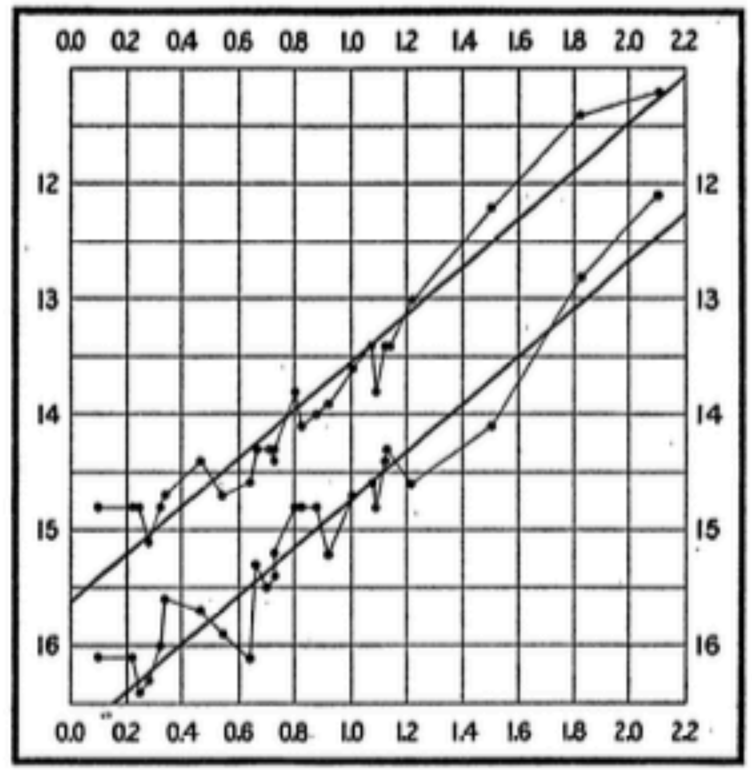


FIG. 2.

# The expanding universe

H. Shapley

# The expanding universe

STUDIES BASED ON THE COLORS AND MAGNITUDES IN STELLAR CLUSTERS[1]

SEVENTH PAPER: THE DISTANCES, DISTRIBUTION IN SPACE, AND DIMENSIONS OF 69 GLOBULAR CLUSTERS

By HARLOW SHAPLEY

I. PARALLAXES FROM VARIABLE STARS, APPARENT MAGNITUDES, AND ANGULAR DIAMETERS

TABLE I

COMPARISON OF CLUSTER PARALLAXES FROM VARIABLES, MAGNITUDES, AND DIAMETERS

| DESIGNATION | | APPARENT DIAMETER | PARALLAX (UNIT IS 0".000001) | | | | RESIDUALS |
|---|---|---|---|---|---|---|---|
| N.G.C. | Messier | | Adopted | From Variables | From Magnitudes | From Diameters | |
| 5272..... | 3 | 7'.0 | 72 | 72 | 71 | 72 | 0, −1, 0 |
| 5904..... | 5 | 8.6 | 80 | 80 | 80 | 81 | 0, 0, +1 |
| 6205..... | 13 | 10.6 | 90 | 82: | 89 | 91 | −8:, −1, +1 |
| 6656..... | 22 | 16.0 | 118 | 116 | 121 | 116 | −2, +3, −2 |
| 7078..... | 15 | 5.0 | 68 | 67 | 69 | 59 | −1, +1, −9 |
| 7089..... | 2 | 7.0 | 64 | 65 | 60 | 72 | +1, −4, +8 |
| 5139..... | ........ | 30 | 153 | 150 | 170: | 155 | −3, +17:, +2 |
| Small Magellanic Cloud.......... | | ........ | 52 | 52 | ........ | ........ | .............. |

# The expanding universe

E.P. Hubble

# The expanding universe

CEPHEIDS IN SPIRAL NEBULAE.

BY EDWIN P. HUBBLE.

Messier 31 and 33, the only spirals that can be seen with the naked eye, have recently been made the subject of detailed investigations with the 100-inch and 60-inch reflectors of the Mount Wilson Observatory. Novae are a common phenomenon in M 31, and Duncan has reported three variables within the area covered by M 33.[1] With these exceptions there seems to have been no definite evidence of actual stars involved in spirals. Under good observing conditions, however, the outer regions of both spirals are resolved into dense swarms of images in no way differing from those of ordinary stars. A survey of the plates made with the blink-comparator has revealed many variables among the stars, a large proportion of which show the characteristic light-curve of the Cepheids.

# The expanding universe

*A RELATION BETWEEN DISTANCE AND RADIAL VELOCITY AMONG EXTRA-GALACTIC NEBULAE*


By Edwin Hubble

Mount Wilson Observatory, Carnegie Institution of Washington



Communicated January 17, 1929


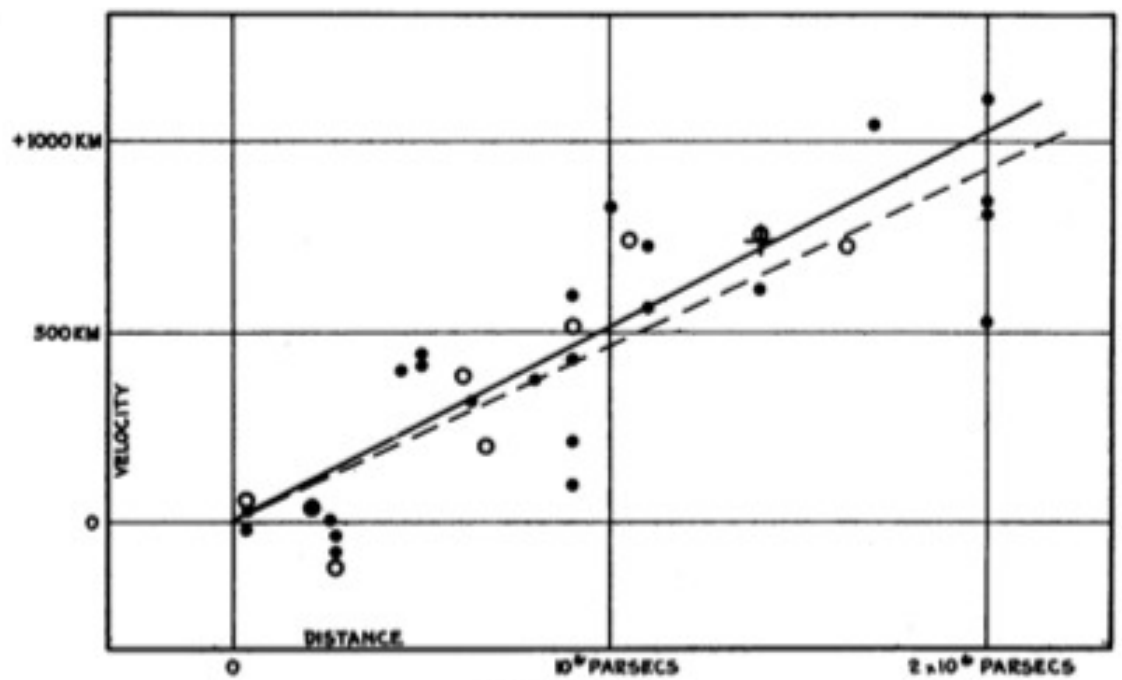


FIGURE 1

Velocity-Distance Relation among Extra-Galactic Nebulae.

$H_0$~500 km/s/Mpc

# Measuring the Hubble rate

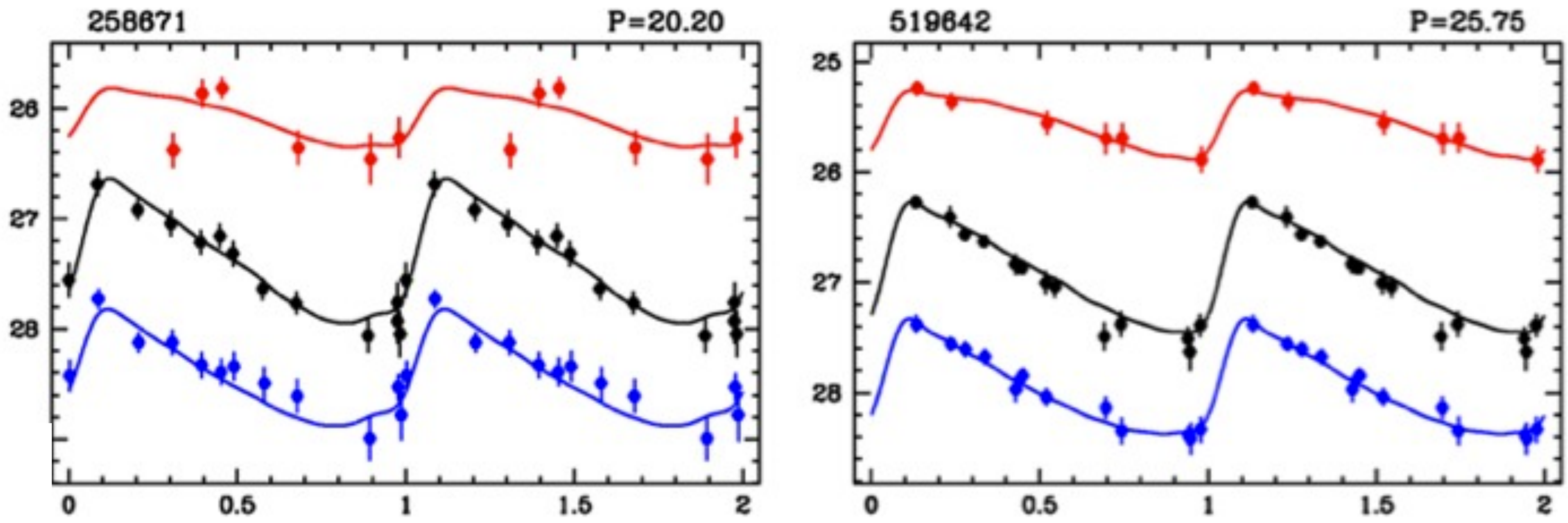


HST Cepheid light curves

# Measuring the Hubble rate

Supernovae as secondary distance indicators

# Measuring the Hubble rate

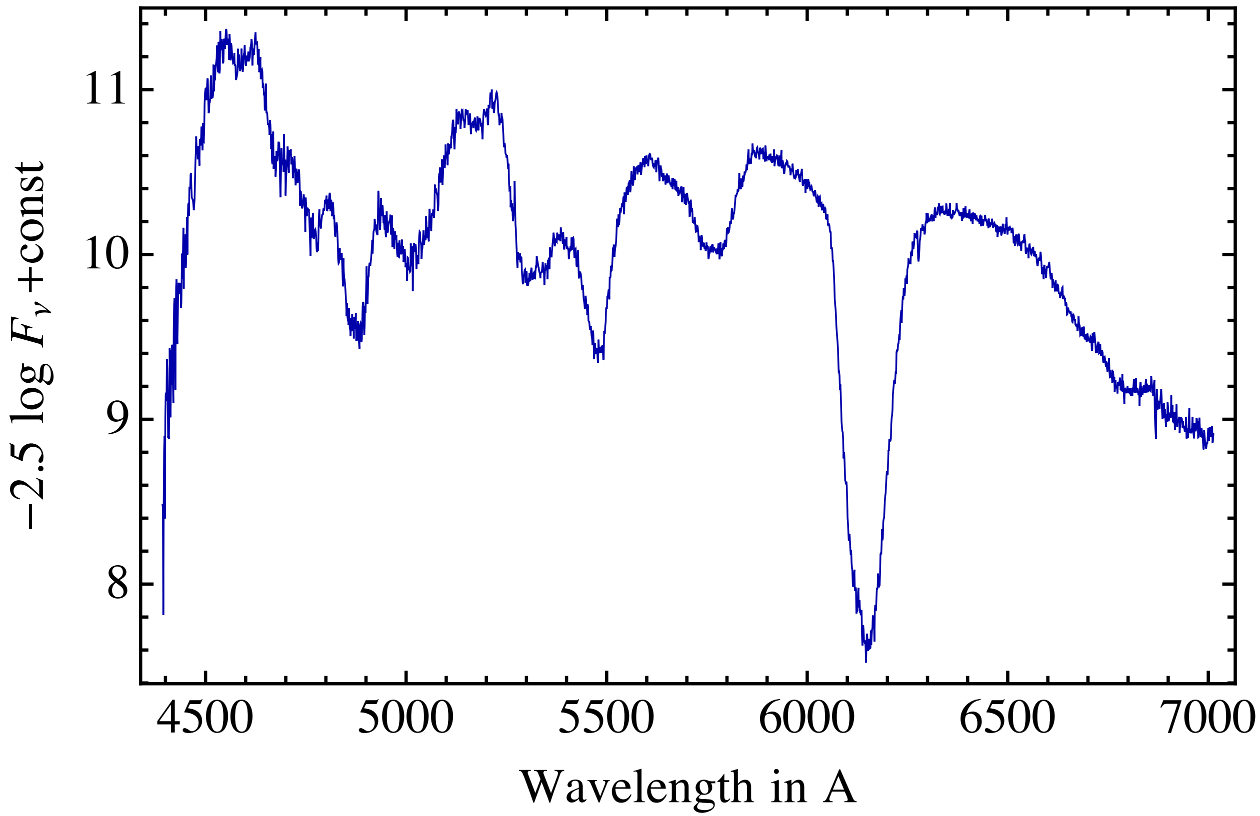


Identification through spectrum

# Measuring the Hubble rate

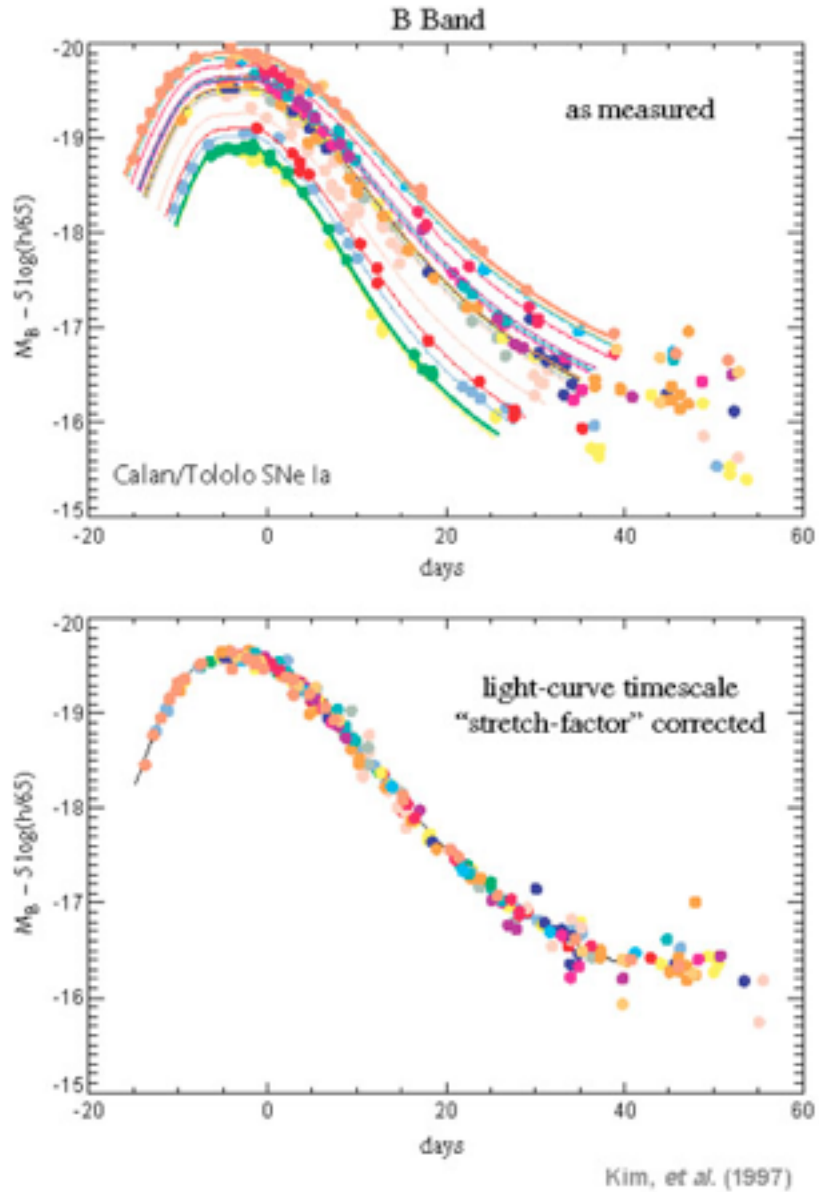


Calibration from light curve

# Measuring the Hubble rate

## Measurement of $H_0$

Measure the luminosity L of a type Ia supernova from 19 nearby supernovae

Then measure $H_0$ from

$$H_0 = \sqrt{\frac{4\pi}{L}} cz\sqrt{F}$$

with $cz\sqrt{F}$ measured from ~300 supernovae

$$H_0 = 73.24 \pm 1.74 \frac{km}{s\,Mpc}$$

**(Riess et al. 2016)**

# Dynamics of the Metric

In general relativity the dynamics of the metric is determined by Einstein's field equations

$$R_{\mu\nu} - \frac{1}{2} g_{\mu\nu} R - g_{\mu\nu} \Lambda = 8\pi G T_{\mu\nu}$$

with

$$R_{\mu\nu} = \frac{\partial \Gamma^{\rho}_{\mu\nu}}{\partial x^{\rho}} - \frac{\partial \Gamma^{\rho}_{\rho\mu}}{\partial x^{\nu}} + \Gamma^{\rho}_{\mu\nu} \Gamma^{\sigma}_{\rho\sigma} - \Gamma^{\rho}_{\mu\sigma} \Gamma^{\sigma}_{\nu\rho} \qquad R = g^{\mu\nu} R_{\mu\nu}$$

$$\Gamma^{\rho}_{\mu\nu} = \frac{1}{2} g^{\rho\sigma} \left( \frac{\partial g_{\sigma\mu}}{\partial x^{\nu}} + \frac{\partial g_{\sigma\nu}}{\partial x^{\mu}} - \frac{\partial g_{\mu\nu}}{\partial x^{\sigma}} \right)$$

and stress tensor $T_{\mu\nu}$

# Dynamics of the Metric

For the flat FLRW universe the stress tensor must be of the form

$$T_{00} = \rho(t)$$

$$T_{0i} = 0$$

$$T_{ij} = a^2 \delta_{ij} p(t)$$

So that Einstein's equations become

$$H^2 = \frac{8\pi G}{3}\rho \qquad \text{(00)}$$

$$3H^2 + 2\dot{H} = -8\pi G p \qquad \text{(ij)}$$

# Dynamics of the Metric

These imply a conservation equation

$$\dot{\rho} + 3H(\rho + p) = 0$$

and we typically use

$$H^2 = \frac{8\pi G}{3}\rho \qquad \text{(Friedmann equation)}$$

$$\dot{\rho} + 3H(\rho + p) = 0 \qquad \text{(Continuity equation)}$$

With two equations for three unknown functions, we need an equation of state $p(\rho)$ to close the system.

# Dynamics of the Metric

## Equation of state for a gas of particles

The action for a collection of particles is

$$S = -\sum_{a=1}^{N} m_a \int d\tau_a \sqrt{-g_{\mu\nu}\dot{x}_a^\mu \dot{x}_a^\nu}$$

this gives rise to the stress tensor

$$T^{\mu\nu} = \sum_{a=1}^{N} \frac{m_a}{\sqrt{-\det g}} \int d\tau_a \delta^4(x - x_a(\tau_a)) \frac{\dot{x}_a^\mu \dot{x}_a^\nu}{\sqrt{-g_{\rho\sigma}\dot{x}_a^\rho \dot{x}_a^\sigma}}$$

# Dynamics of the Metric

or after integration over the affine parameters

$$T^{\mu\nu} = \sum_{a=1}^{N} \frac{1}{\sqrt{-\det g}} \delta^3(x^i - x^i_a(t)) \frac{p^\mu_a p^\nu_a}{p^0_a}$$

with

$$p^0_a = \sqrt{g^{ij} p_{i\,a} p_{j\,a} + m^2_a}$$

# Dynamics of the Metric

For a given species of particles $m_a = m$

$$T^{\mu\nu} = \int \frac{d^3p}{\sqrt{-\det g}} n(x^i, p_j, t) \frac{p^\mu p^\nu}{p^0}$$

with

$$p^0 = \sqrt{g^{ij} p_i p_j + m^2}$$

and phase space density

$$n(x^i, p_j, t) = \sum_{a=1}^{N} \delta^3(x^i - x^i_a(t)) \delta^3(p_j - p_{j\,a}(t))$$

# Dynamics of the Metric

The symmetries of FLRW imply

$$n(x^i, p_j, t) = n(p, t) \qquad \text{with} \qquad p = \sqrt{\delta^{ij} p_i p_j}$$

so that the stress tensor is given by

$$T^{\mu\nu} = \int \frac{d^3p}{a^3} n(p,t) \frac{p^\mu p^\nu}{\sqrt{(p/a)^2 + m^2}}$$

As expected $T^{0i} = 0$, and

$$\rho(t) = \int \frac{d^3p}{a^3} n(p,t) \sqrt{(p/a)^2 + m^2}$$

$$p(t) = \frac{1}{3a^2} \int \frac{d^3p}{a^3} n(p,t) \frac{p^2}{\sqrt{(p/a)^2 + m^2}}$$

# Dynamics of the Metric

Non-relativistic particles

$$n(p,t) \approx 0 \quad \text{unless} \quad p/a \ll m$$

Then

$$\rho(t) = \int \frac{d^3p}{a^3} n(p,t) m + \ldots$$

$$p(t) = \frac{1}{3} \int \frac{d^3p}{a^3} n(p,t) \frac{(p/a)^2}{m} \ll \rho(t)$$

or

$$\rho = mn$$

$$p \approx 0$$

# Dynamics of the Metric

<u>Relativistic particles</u>

Integration dominated by $p/a \gg m$

Then

$$\rho(t) = \int \frac{d^3p}{a^3} n(p,t) \frac{p}{a}$$

$$p(t) = \frac{1}{3} \int \frac{d^3p}{a^3} n(p,t) \frac{p}{a} = \frac{1}{3}\rho(t)$$

or

$$p(t) = \frac{1}{3}\rho(t)$$

# Dynamics of the Metric

Vaccum energy

$$T_{\mu\nu} = -\rho_V g_{\mu\nu}$$

or

$$T_{00} = \rho_V$$

$$T_{ij} = -a^2 \delta_{ij} \rho_V$$

so that

$$p_V = -\rho_V$$

# Dynamics of the Metric

Typically, the equation of state is taken as

$$p = w\rho$$

The continuity equation then leads to

$$\rho(t) = \rho(t_0)\left(\frac{a(t_0)}{a(t)}\right)^{3(1+w)}$$

with

$$\begin{aligned} w &= 0 && \text{for pressureless dust,} \\ w &= \tfrac{1}{3} && \text{for radiation,} \\ w &= -1 && \text{for vacuum energy.} \end{aligned}$$

# Dynamics of the Metric

For a situation with more than one component

$$H^2 = \frac{8\pi G}{3}\left(\rho_M + \rho_R + \rho_\Lambda\right)$$

with

| | | |
|---|---|---|
| $\rho_M = \Omega_M \rho_{\mathrm{crit},0} \left(\frac{a_0}{a}\right)^3$ | $(p = 0)$ | matter |
| $\rho_R = \Omega_R \rho_{\mathrm{crit},0} \left(\frac{a_0}{a}\right)^4$ | $(p = \frac{1}{3}\rho)$ | radiation |
| $\rho_\Lambda = \Omega_\Lambda \rho_{\mathrm{crit},0}$ | $(p = -\rho)$ | cosmological constant |

# Dark Matter

Fritz Zwicky

# Dark Matter

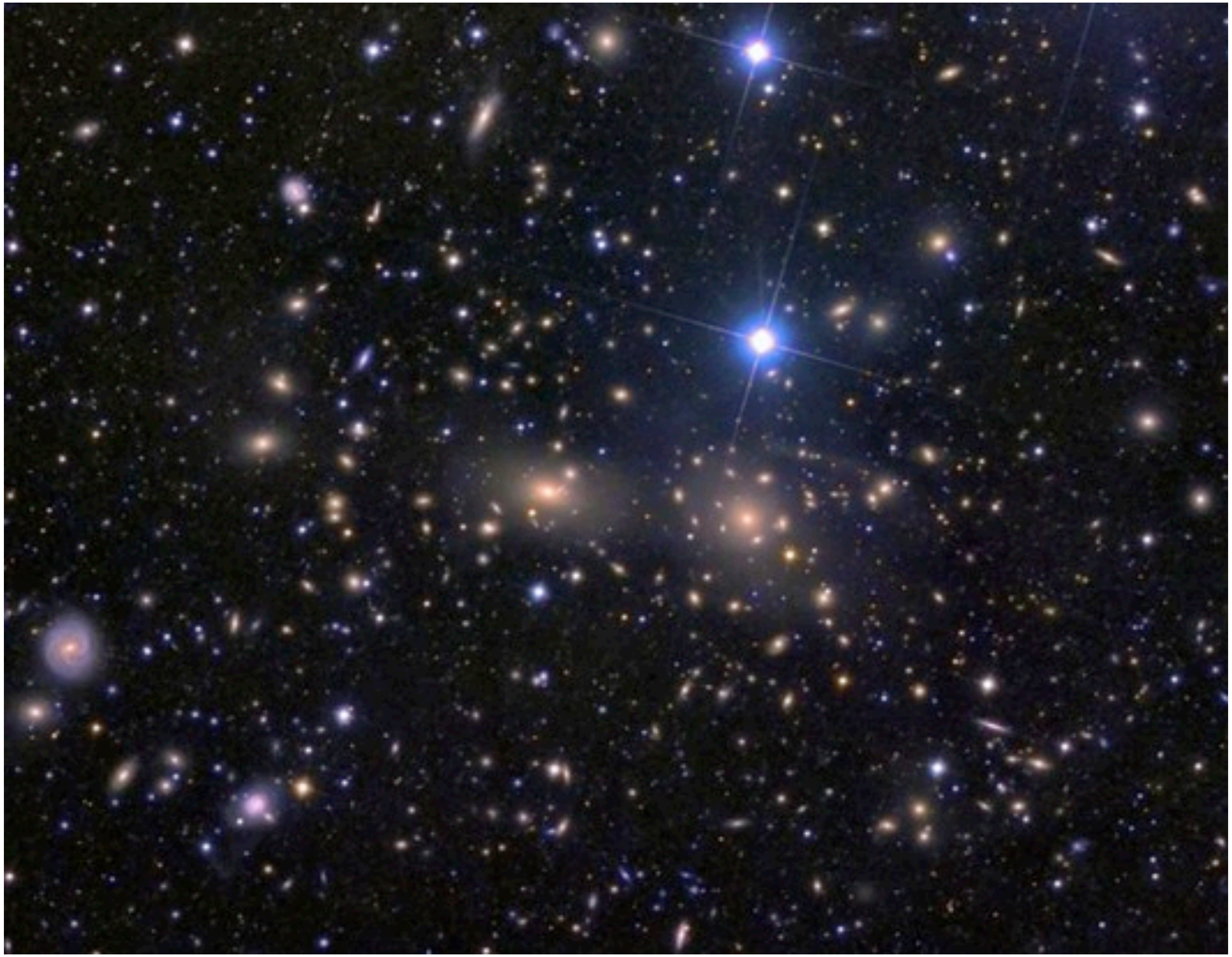

Coma cluster

# Dark Matter

## Die Rotverschiebung von extragalaktischen Nebeln

von **F. Zwicky.**

(16. II. 33.)

*Inhaltsangabe.* Diese Arbeit gibt eine Darstellung der wesentlichsten Merkmale extragalaktischer Nebel, sowie der Methoden, welche zur Erforschung derselben gedient haben. Insbesondere wird die sog. Rotverschiebung extragalaktischer Nebel eingehend diskutiert. Verschiedene Theorien, welche zur Erklärung dieses wichtigen Phänomens aufgestellt worden sind, werden kurz besprochen. Schliesslich wird angedeutet, inwiefern die Rotverschiebung für das Studium der durchdringenden Strahlung von Wichtigkeit zu werden verspricht.

# Dark Matter

Tabelle II[1]).

| Nebelhaufen | Zahl d. Nebel im Haufen | Scheinbarer Durchmesser | Entfernung in $10^6$ Licht-jahren | Mittlere Geschwin-digkeit km/sek |
|---|---|---|---|---|
| Virgo . . . | (500) | 12° | 6 | 890 |
| Pegasus . . | 100 | 1° | 23,6 | 3810 |
| Pisces . . . | 20 | 0,5 | 22,8 | 4630 |
| Cancer . . | 150 | 1,5 | 29,3 | 4820 |
| Perseus . . | 500 | 2,0 | 36 | 5230 |
| Coma . . . | 800 | 1,7 | 45 | 7500 |
| Ursa Major I | 300 | 0,7 | 72 | 11800 |
| Leo . . . . | 400 | 0,6 | 104 | 19600 |
| Gemini . . | (300) | — | 135 | 23500 |

Diese Resultate sind in Fig. 2 graphisch dargestellt.

# Dark Matter

## Virial Theorem

Consider a system of particles

$$m_a \ddot{\mathbf{r}}_a = -\nabla_a V(\mathbf{r}_1, \ldots, \mathbf{r}_N)$$

This implies

$$\sum_a m_a \mathbf{r}_a \cdot \ddot{\mathbf{r}}_a = -\sum_a \mathbf{r}_a \cdot \nabla_a V(\mathbf{r}_1, \ldots, \mathbf{r}_N)$$

and for a homogeneous function of degree n

$$V(\lambda \mathbf{r}_1, \ldots, \lambda \mathbf{r}_N) = \lambda^n V(\mathbf{r}_1, \ldots, \mathbf{r}_N)$$

$$\sum_a m_a \mathbf{r}_a \cdot \ddot{\mathbf{r}}_a = -n V(\mathbf{r}_1, \ldots, \mathbf{r}_N)$$

# Dark Matter

Writing

$$\sum_a m_a \mathbf{r}_a \cdot \ddot{\mathbf{r}}_a = \frac{1}{2}\frac{d^2}{dt^2}\sum_a m_a \mathbf{r}_a^2 - 2T$$

for gravitational interactions this gives

$$2T + V = -\frac{1}{2} M \frac{d^2}{dt^2}\langle \mathbf{r}^2 \rangle$$

In virial equilibrium

$$2T + V = 0$$

# Dark Matter

For a virialized cluster of galaxies, we expect

$$\langle \mathbf{v^2} \rangle = GM \left\langle \frac{1}{r} \right\rangle$$

where M is the total mass of all galaxies.

For Coma, Zwicky estimated

$$\langle \mathbf{v^2} \rangle \simeq 80 \frac{\mathrm{km}}{\mathrm{s}}$$

yet the observed dispersion is

$$\langle \mathbf{v^2} \rangle \simeq 900 \frac{\mathrm{km}}{\mathrm{s}}$$

# Dark Matter

*Scheinbare Geschwindigkeiten im Comahaufen.*

| | |
|---|---|
| $v =$ 8500 km/sek | 6900 km/sek |
| 7900 | 6700 |
| 7600 | 6600 |
| 7000 | 5100 (?) |

Um, wie beobachtet, einen mittleren Dopplereffekt von 1000 km/sek oder mehr zu erhalten, müsste also die mittlere Dichte im Comasystem mindestens 400 mal grösser sein als die auf Grund von Beobachtungen an leuchtender Materie abgeleitete[1]). Falls sich dies bewahrheiten sollte, würde sich also das überraschende Resultat ergeben, dass dunkle Materie in sehr viel grösserer Dichte vorhanden ist als leuchtende Materie.

# Dark Matter

Rotation curves

Vera Rubin

# Dark Matter

Vera Rubin measured the radial velocities of stars (and HII regions) in edge-on spiral galaxies

According to Newton

$$v^2(r) = \frac{GM(r)}{r}$$

Beyond the disk we expect

$$M(r) \approx M_{\rm disk}$$

or

$$v^2(r) = \frac{GM_{\rm disk}}{r}$$

# Dark Matter

ROTATION OF THE ANDROMEDA NEBULA FROM A SPECTROSCOPIC SURVEY OF EMISSION REGIONS*

VERA C. RUBIN† AND W. KENT FORD, JR.†
Department of Terrestrial Magnetism, Carnegie Institution of Washington and Lowell Observatory, and Kitt Peak National Observatory‡
*Received 1969 July 7; revised 1969 August 21*

ABSTRACT

Spectra of sixty-seven H II regions from 3 to 24 kpc from the nucleus of M31 have been obtained with the DTM image-tube spectrograph at a dispersion of 135 Å $mm^{-1}$. Radial velocities, principally from $H\alpha$, have been determined with an accuracy of $\pm 10$ km $sec^{-1}$ for most regions. Rotational velocities have been calculated under the assumption of circular motions only.

For the region interior to 3 kpc where no emission regions have been identified, a narrow [N II] $\lambda 6583$ emission line is observed. Velocities from this line indicate a rapid rotation in the nucleus, rising to a maximum circular velocity of $V = 225$ km $sec^{-1}$ at $R = 400$ pc, and falling to a deep minimum near $R = 2$ kpc.

From the rotation curve for $R \leq 24$ kpc, the following disk model of M31 results. There is a dense, rapidly rotating nucleus of mass $M = (6 \pm 1) \times 10^9 M_\odot$. Near $R = 2$ kpc, the density is very low and the rotational motions are very small. In the region from 500 to 1.4 kpc (most notably on the southeast minor axis), gas is observed leaving the nucleus. Beyond $R = 4$ kpc the total mass of the galaxy increases approximately linearly to $R = 14$ kpc, and more slowly thereafter. The total mass to $R = 24$ kpc is $M = (1.85 \pm 0.1) \times 10^{11} M_\odot$; one-half of it is located in the disk interior to $R = 9$ kpc. In many respects this model resembles the model of the disk of our Galaxy. Outside the nuclear region, there is no evidence for noncircular motions.

The optical velocities, $R > 3$ kpc, agree with the 21-cm observations, although the maximum rotational velocity, $V = 270 \pm 10$ km $sec^{-1}$, is slightly higher than that obtained from 21-cm observations.

# Dark Matter

M31

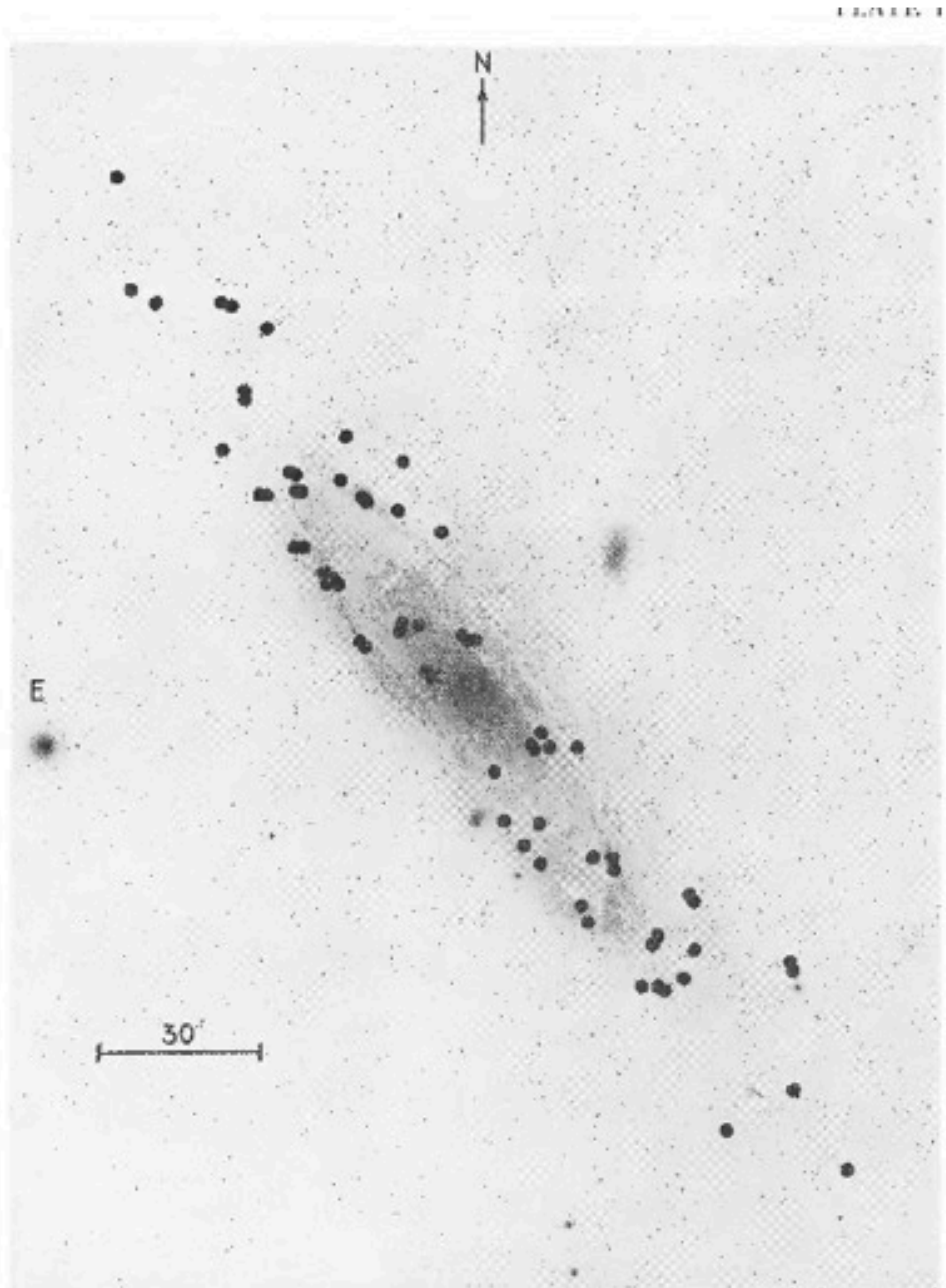

# Dark Matter

M31

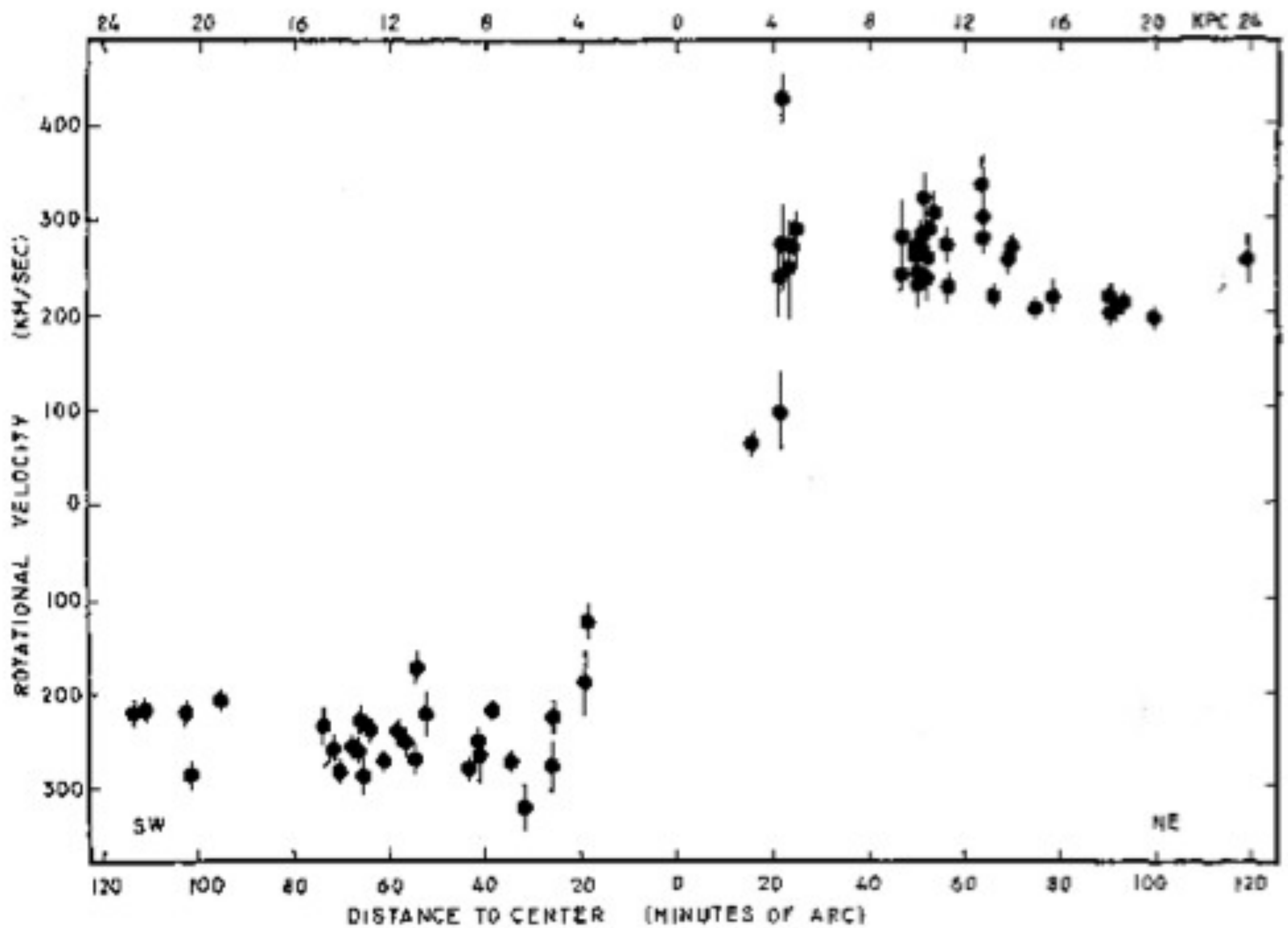

# Dark Matter

## ROTATIONAL PROPERTIES OF 21 Sc GALAXIES WITH A LARGE RANGE OF LUMINOSITIES AND RADII, FROM NGC 4605 ($R = 4$ kpc) TO UGC 2885 ($R = 122$ kpc)

VERA C. RUBIN,[1,2] W. KENT FORD, JR.,[1] AND NORBERT THONNARD
Department of Terrestrial Magnetism, Carnegie Institution of Washington
*Received 1979 October 11; accepted 1979 November 29*

### ABSTRACT

For 21 Sc galaxies whose properties encompass a wide range of radii, masses, and luminosities, we have obtained major axis spectra extending to the faint outer regions, and have deduced rotation curves. The galaxies are of high inclination, so uncertainties in the angle of inclination to the line of sight and in the position angle of the major axis are minimized. Their radii range from 4 to 122 kpc ($H = 50$ km s$^{-1}$ Mpc$^{-1}$); in general, the rotation curves extend to 83% of $R_{25}{}^{i,b}$. When plotted on a linear scale with no scaling, the rotation curves for the smallest galaxies fall upon the initial parts of the rotation curves for the larger galaxies. All curves show a fairly rapid velocity rise to $V \sim 125$ km s$^{-1}$ at $R \sim 5$ kpc, and a slower rise thereafter. Most rotation curves are rising slowly even at the farthest measured point. Neither high nor low luminosity Sc galaxies have falling rotation curves. Sc galaxies of all luminosities must have significant mass located beyond the optical image. A linear relation between log $V_{max}$ and log $R$ follows from the shape of the common rotation curve for all Sc's, and the tendency of smaller galaxies, at any $R$, to have lower velocities than the large galaxies at that $R$. The significantly shallower slope discovered for this relation by Tully and Fisher is attributed to their use of galaxies of various Hubble types and the known correlation of $V_{max}$ with Hubble type.

# Dark Matter

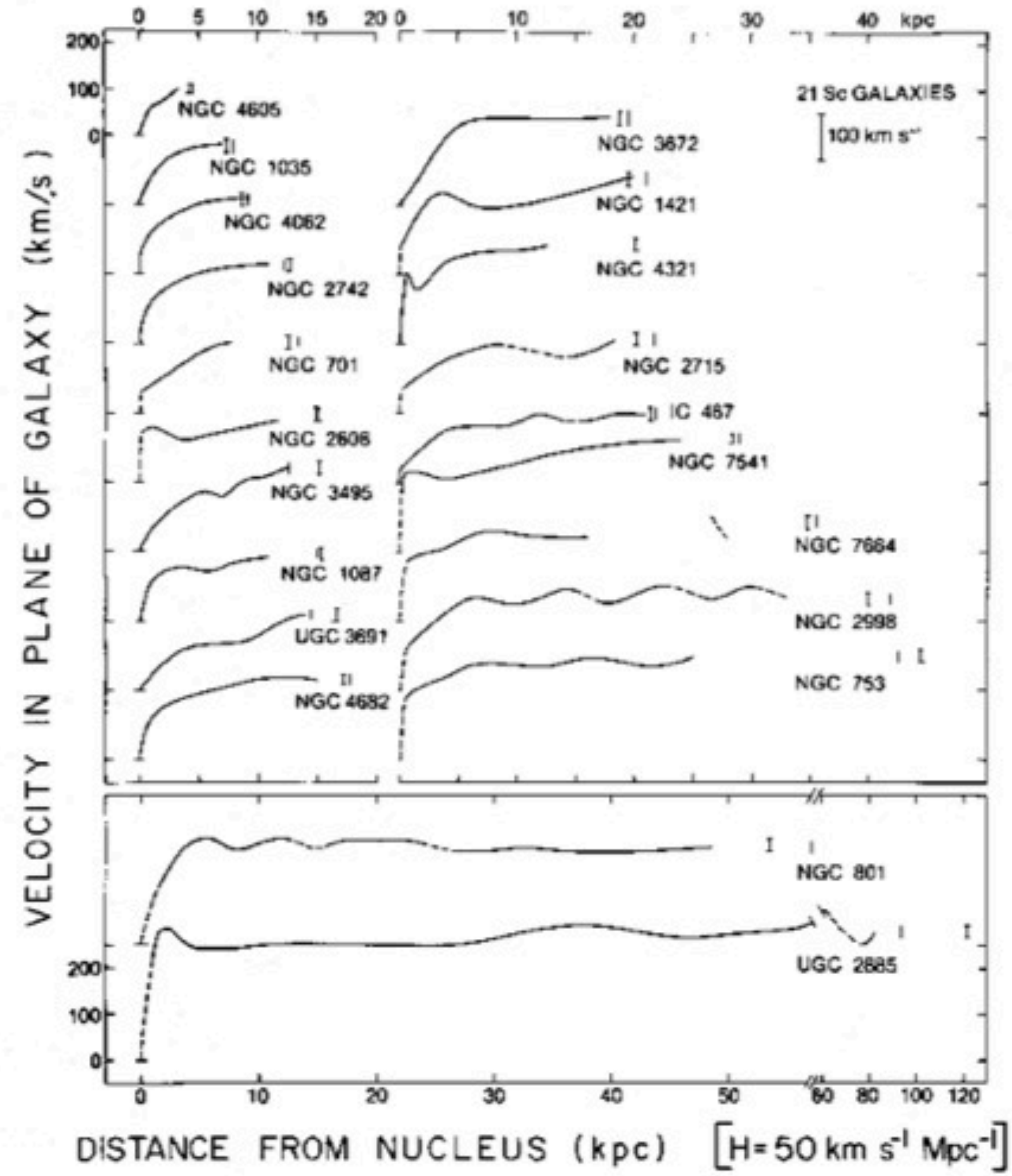

21 Sc GALAXIES
100 km s⁻¹
NGC 4605
NGC 1035
NGC 4062
NGC 2742
NGC 701
NGC 2608
NGC 3495
NGC 1087
UGC 3691
NGC 4682
NGC 3672
NGC 1421
NGC 4321
NGC 2715
IC 467
NGC 7541
NGC 7664
NGC 2998
NGC 753
NGC 801
UGC 2885
VELOCITY IN PLANE OF GALAXY (km/s)
DISTANCE FROM NUCLEUS (kpc) [H=50 km s⁻¹ Mpc⁻¹]
kpc

# Dark Matter

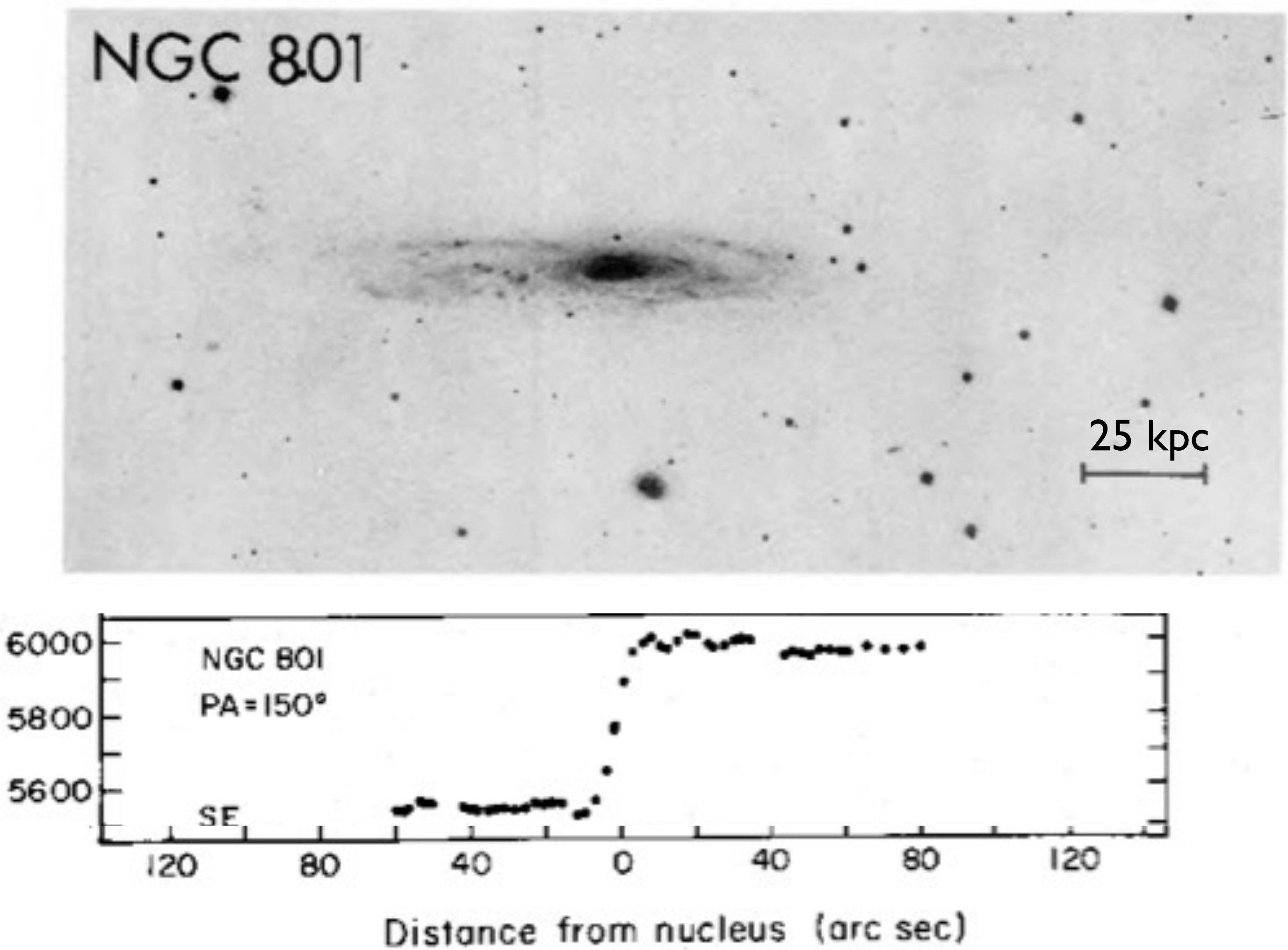

NGC 801
25 kpc
6000
5800
5600
NGC 801
PA = 150°
SE
120
80
40
0
40
80
120
Distance from nucleus (arc sec)

# Dark Matter

Spirals in numerical simulations

Jerry Ostriker

Jim Peebles

# Dark Matter

## A NUMERICAL STUDY OF THE STABILITY OF FLATTENED GALAXIES: OR, CAN COLD GALAXIES SURVIVE?*

J. P. OSTRIKER
Princeton University Observatory

AND

P. J. E. PEEBLES
Joseph Henry Laboratories, Princeton University
*Received 1973 May 29*

ABSTRACT

To study the stability of flattened galaxies, we have followed the evolution of simulated galaxies containing 150 to 500 mass points. Models which begin with characteristics similar to the disk of our Galaxy (except for increased velocity dispersion and thickness to assure local stability) were found to be rapidly and grossly unstable to barlike modes. These modes cause an increase in random kinetic energy, with approximate stability being reached when the ratio of kinetic energy of rotation to total gravitational energy, designated $t$, is reduced to the value of $0.14 \pm 0.02$. Parameter studies indicate that the result probably is not due to inadequacies of the numerical $N$-body simulation method. A survey of the literature shows that a critical value for limiting stability $t \simeq 0.14$ has been found by a variety of methods.

Models with added spherical (halo) component are more stable. It appears that halo-to-disk mass ratios of 1 to $2\frac{1}{2}$, and an initial value of $t \simeq 0.14 \pm 0.03$, are required for stability. If our Galaxy (and other spirals) do not have a substantial unobserved mass in a hot disk component, then apparently the halo (spherical) mass *interior* to the disk must be comparable to the disk mass. Thus normalized, the halo masses of our Galaxy and of other spiral galaxies *exterior* to the observed disks may be extremely large.

# Dark Matter

X-ray observations of clusters

The gas in a galaxy cluster between galaxies is expected to emit X-rays.

$$v^2 = \frac{GM}{R} \sim (10^{-3}c)^2$$

So protons carry kinetic energies of a few keV and we expect X-ray photons to emitted in collisions.

$$L_X(r) = \Lambda(T_b(r))\rho_b^2(r)$$

# Dark Matter

In hydrostatic equilibrium we expect pressure and gravitational force to balance each other

$$\frac{dp_b}{dr} = -\frac{4\pi G\rho_b(r)}{r^2}\int_0^r dr' {r'}^2 \rho_m(r')$$

We must specify some equation of state. For ideal gas

$$p_b = \rho_b T_b / m_b$$

so that

$$\frac{d}{dr}\frac{r^2}{\rho_b(r)}\frac{d}{dr}\left(\frac{\rho_b(r)T_b(r)}{m_b}\right) = -4\pi G r^2 \rho_m(r)$$

# Dark Matter

In principle both density and temperature are observable, but the cluster is often assumed to be isothermal

$$\frac{d}{dr}\frac{r^2}{\rho_b(r)}\frac{d\rho_b(r)}{dr} = -\frac{4\pi G r^2}{\sigma_b^2}\rho_m(r)$$

with

$$\frac{T_b(r)}{m_b} = \sigma_b^2$$

Assuming further that dark and baryonic matter have the same profile

$$\frac{\rho_b(r)}{\rho_b(0)} = \frac{\rho_m(r)}{\rho_m(0)} = F(r)$$

# Dark Matter

we have

$$\frac{d}{dr}\frac{r^2}{F(r)}\frac{dF(r)}{dr} = -9\frac{r^2}{r_c^2}F(r)$$

with core radius

$$r_c = \sqrt{\frac{9\sigma_b^2}{4\pi G\rho_m(0)}}$$

Because $F(0) = 1$ by definition and $F'(0) = 0$ by analyticity, the core radius is the only parameter of the profile.

A measurement of the core radius from the image and temperature from the spectrum then gives $\rho_m(0)$, and the luminosity determines $\rho_b(0)$.

# Dark Matter

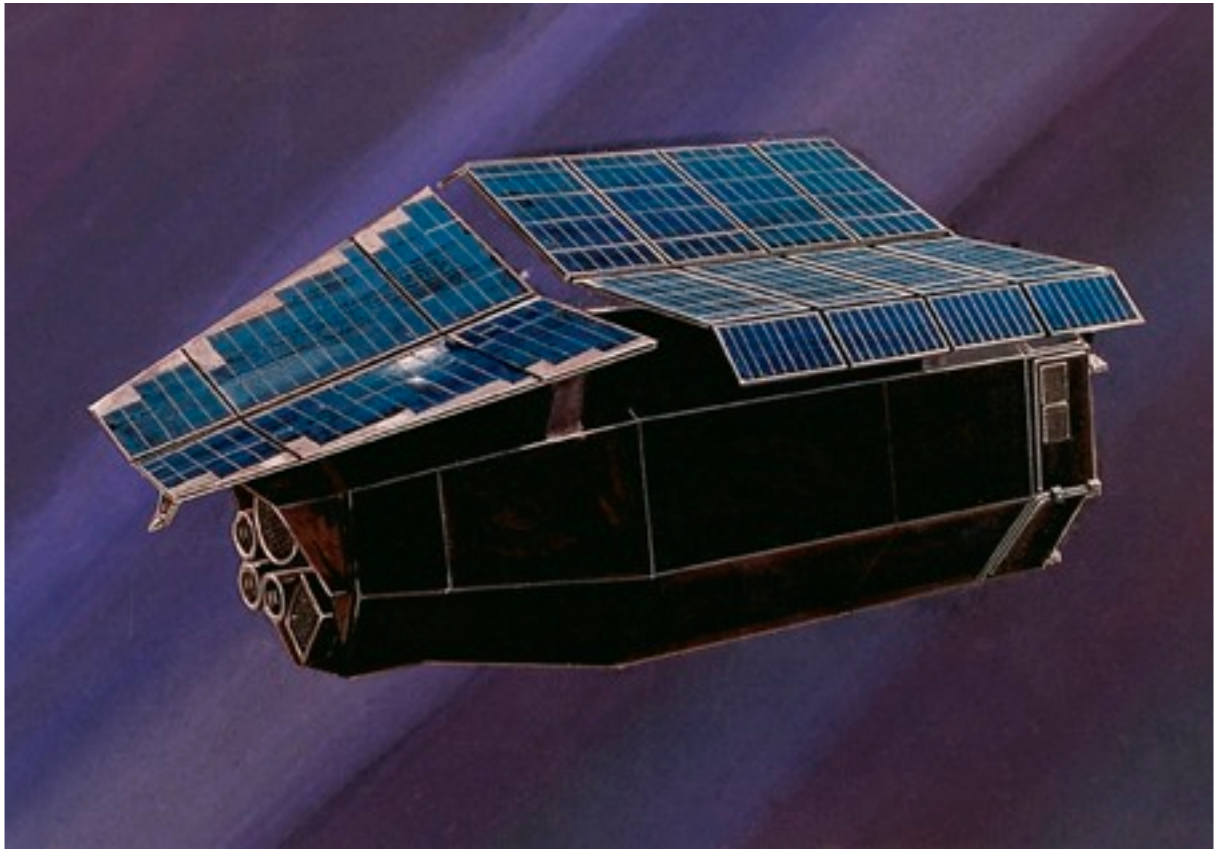

Einstein Observatory

# Dark Matter

THE STRUCTURE OF CLUSTERS OF GALAXIES OBSERVED WITH *EINSTEIN*

C. JONES AND W. FORMAN
Harvard-Smithsonian Center for Astrophysics
*Received 1982 November 1; accepted 1983 June 13*

ABSTRACT

We have used *Einstein* imaging observations to study the structure of clusters of galaxies. We have produced surface brightness profiles of the X-ray emission from 46 clusters of galaxies. By fitting these profiles to hydrostatic-isothermal models of the intracluster gas, we have determined the X-ray luminosity and derived the cluster core radius, the ratio of the scale height of the galaxies to that of the gas, and the central gas density. This analysis of these X-ray observations shows that clusters of galaxies can be divided into two families based on their core radii which characterize the clusters' total gravitational potential and the presence or absence of a central bright galaxy. Clusters in the XD family have small core radii ($\lesssim$300 kpc) with the X-ray emission centered on a central, stationary, optically dominant galaxy. Clusters classed nXD have larger core radii ($\sim$400 to $\sim$800 kpc), and generally the emission is not centered on a stationary, bright galaxy. Clusters in both families exhibit a wide range of dynamical properties; we conclude from this that the formation of a central, dominant galaxy occurs in the early stages of cluster collapse. Nearly half of the clusters in the XD family show central emission in excess of that expected from fitting the hydrostatic-isothermal model to the outer regions of the cluster. The derived gas densities and temperatures for these clusters are consistent with those expected if the central excesses are produced by cooling accretion flows. In addition, a correlation is found between the X-ray luminosities of the central excess and the radio luminosities of core sources, which supports the suggestion that cooling flows power the core radio sources.

The X-ray surface brightness profiles show that in general there is more energy per unit mass in the cluster gas than in the galaxies (i.e., the scale height of the gas exceeds that of the galaxies). The determinations of the gas and galaxy scale heights from the X-ray gas temperatures and the cluster velocity dispersions support this conclusion. We discuss briefly the possibility that a hot intercluster medium could heat the intracluster gas and thereby increase its scale height relative to that of the galaxies.

*Subject headings:* galaxies: clustering — galaxies: intergalactic medium — X-rays: sources

# Dark Matter

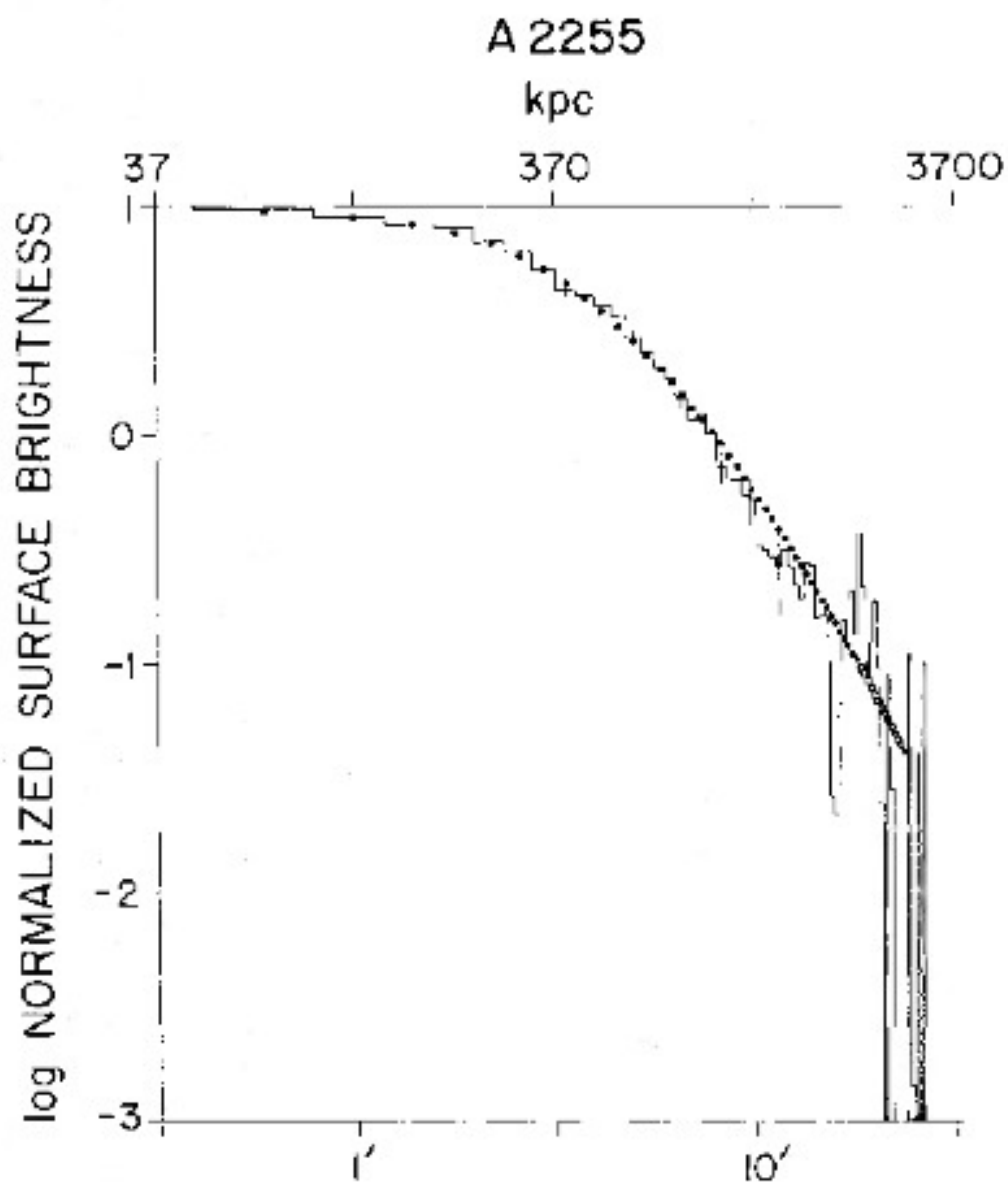
A 2255
kpc
37
370
3700
log NORMALIZED SURFACE BRIGHTNESS
1
0
-1
-2
-3
1′
10′

# Dark Matter

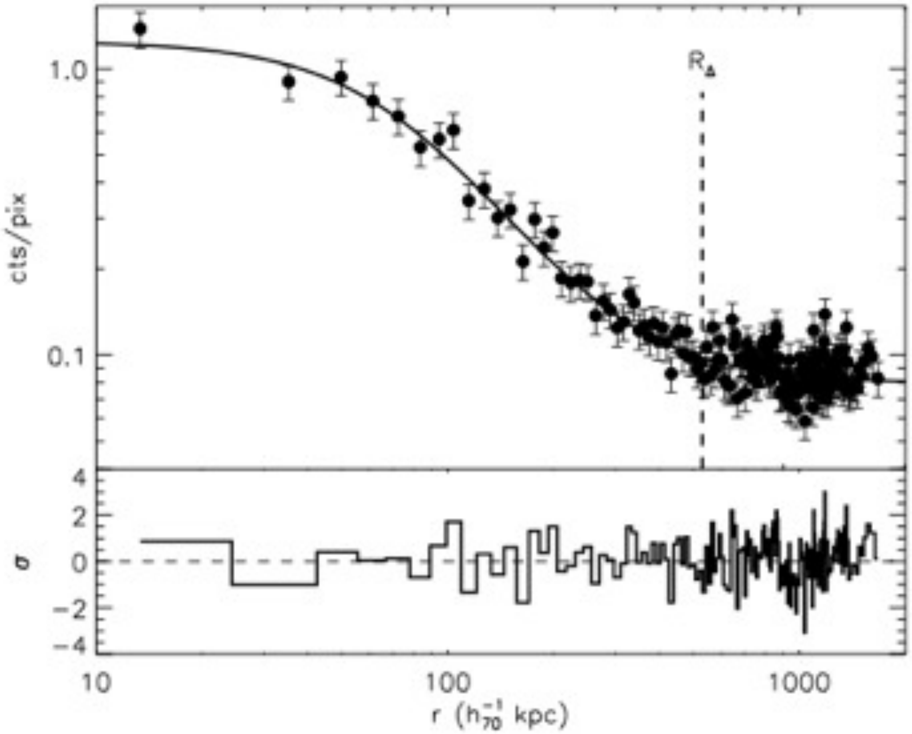


Chandra

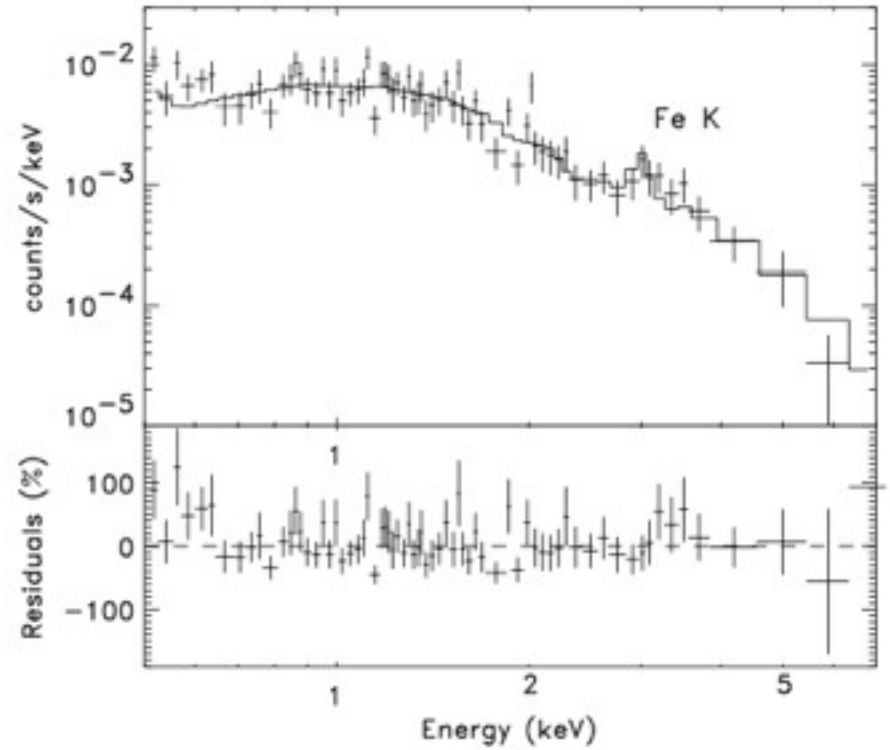


XMM Newton

# Dark Matter

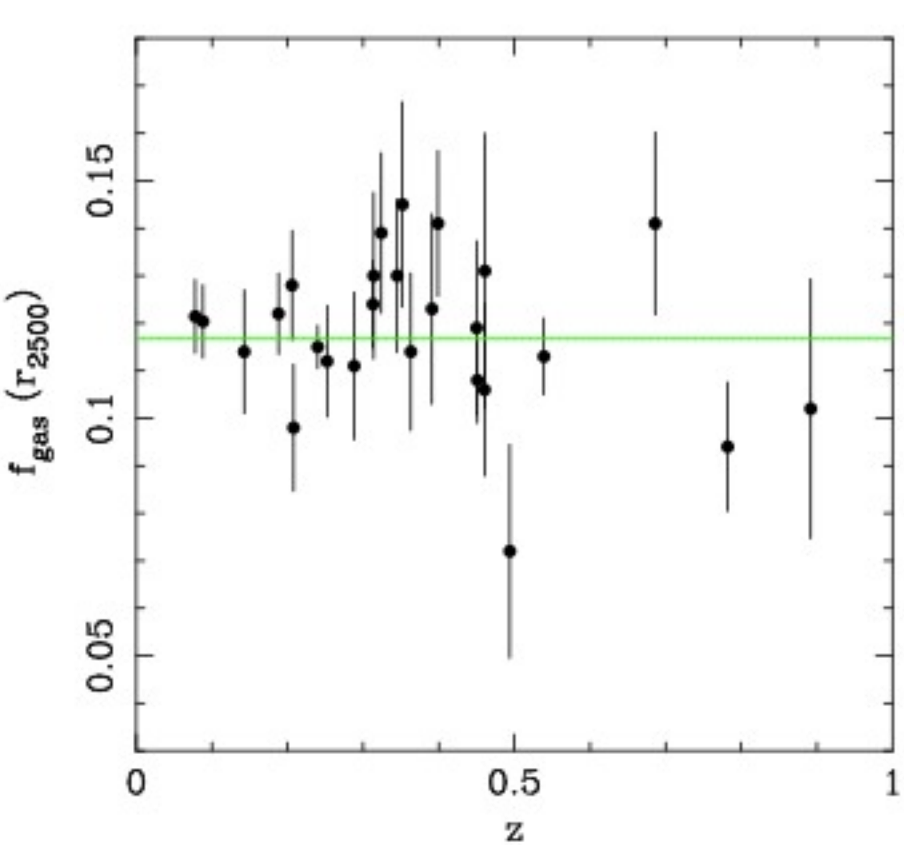


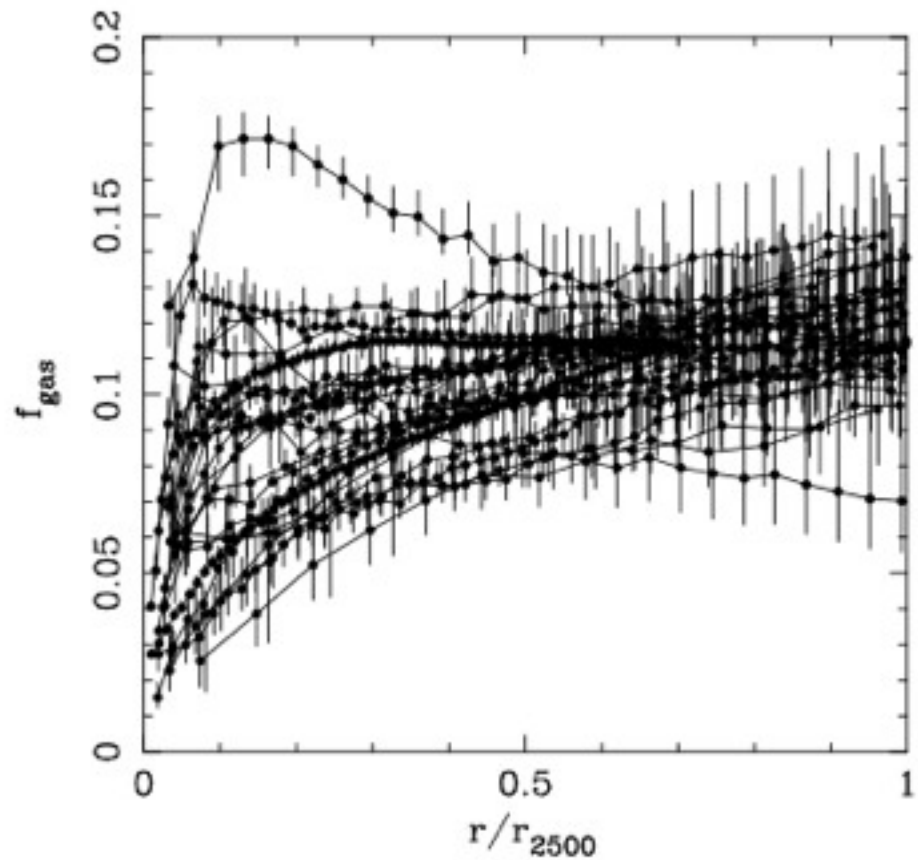


The hot gas fraction is much less than unity

# Dark Energy

Measurements of the shape of the luminosity distance

$$d_L(z) = a_0 r(1+z)$$

allow us to further constrain the composition of the universe.

With

$$r = \int_t^{t_0} \frac{dt'}{a(t')}$$

and

$$dt = \frac{da}{aH} = -\frac{dz}{(1+z)H}$$

we have

$$d_L(z) = (1+z)\int_0^z \frac{dz'}{H(z')}$$

# Dark Energy

Together with the Friedmann equation

$$d_L(z) = \frac{1+z}{H_0} \int_0^z \frac{dz'}{\sqrt{\Omega_\Lambda + \Omega_K(1+z')^2 + \Omega_m(1+z')^3 + \Omega_r(1+z')^4}}$$

The Hubble parameter only enters as an overall factor, the shape depends on the composition of the universe

# Dark Energy

Supernova Cosmology Project

# Dark Energy

**Measurements of the Cosmological Parameters $\Omega$ and $\Lambda$ from the First 7 Supernovae at $z \geq 0.35$**[*]

S. Perlmutter,[1,2] S. Gabi,[1,3] G. Goldhaber,[1,2] A. Goobar,[1,2,4] D. E. Groom,[1,2] I. M. Hook,[2,10] A. G. Kim,[1,2] M. Y. Kim,[1] J. C. Lee,[1] R. Pain,[1,5] C. R. Pennypacker,[1,3] I. A. Small,[1,2] R. S. Ellis,[6] R. G. McMahon,[6] B. J. Boyle,[7,8] P. S. Bunclark,[7] D. Carter,[7] M. J. Irwin,[7] K. Glazebrook,[8] H. J. M. Newberg,[9] A. V. Filippenko,[2,10] T. Matheson,[10] M. Dopita,[11] and W. J. Couch[12]
(The Supernova Cosmology Project)

We have developed a technique to systematically discover and study high-redshift supernovae that can be used to measure the cosmological parameters. We report here results based on the initial seven of >28 supernovae discovered to date in the high-redshift supernova search of the Supernova Cosmology Project. We find an observational dispersion in peak magnitudes of $\sigma_{M_B} = 0.27$; this dispersion narrows to $\sigma_{M_B,\mathrm{corr}} = 0.19$ after "correcting" the magnitudes using the light-curve "width-luminosity" relation found for nearby ($z \leq 0.1$) type Ia supernovae from the Calán/Tololo survey (Hamuy *et al.* 1996). Comparing lightcurve-width-corrected magnitudes as a function of redshift of our distant ($z = 0.35$–$0.46$) supernovae to those of nearby type Ia supernovae yields a global measurement of the mass density, $\Omega_{\mathrm{M}} = 0.88\ ^{+0.69}_{-0.60}$ for a $\Lambda = 0$ cosmology. For a spatially flat universe (i.e., $\Omega_{\mathrm{M}} + \Omega_\Lambda = 1$), we find $\Omega_{\mathrm{M}} = 0.94\ ^{+0.34}_{-0.28}$ or, equivalently, a measurement of the cosmological constant, $\Omega_\Lambda = 0.06\ ^{+0.28}_{-0.34}$ (<0.51 at the 95% confidence level).

August 1996

# Dark Energy

High-z Supernova Search Team

# Observational Evidence from Supernovae for an Accelerating Universe and a Cosmological Constant

Adam G. Riess[1], Alexei V. Filippenko[1], Peter Challis[2], Alejandro Clocchiatti[3], Alan Diercks[4], Peter M. Garnavich[2], Ron L. Gilliland[5], Craig J. Hogan[4], Saurabh Jha[2], Robert P. Kirshner[2], B. Leibundgut[6], M. M. Phillips[7], David Reiss[4], Brian P. Schmidt[8] [9], Robert A. Schommer[7], R. Chris Smith[7] [10], J. Spyromilio[6], Christopher Stubbs[4], Nicholas B. Suntzeff[7], John Tonry[11]

We present spectral and photometric observations of 10 type Ia supernovae (SNe Ia) in the redshift range $0.16 \leq z \leq 0.62$. The luminosity distances of these objects are determined by methods that employ relations between SN Ia luminosity and light curve shape. Combined with previous data from our High-Z Supernova Search Team (Garnavich et al. 1998; Schmidt et al. 1998) and Riess et al. (1998a), this expanded set of 16 high-redshift supernovae and a set of 34 nearby supernovae are used to place constraints on the following cosmological parameters: the Hubble constant ($H_0$), the mass density ($\Omega_M$), the cosmological constant (i.e., the vacuum energy density, $\Omega_\Lambda$), the deceleration parameter ($q_0$), and the dynamical age of the Universe ($t_0$). The distances of the high-redshift SNe Ia are, on average, 10% to 15% farther than expected in a low mass density ($\Omega_M = 0.2$) Universe without a cosmological constant. Different light curve fitting methods, SN Ia subsamples, and prior constraints unanimously favor eternally expanding models with positive cosmological constant (i.e., $\Omega_\Lambda > 0$) and a current acceleration of the expansion (i.e., $q_0 < 0$). With no prior constraint on mass density other than $\Omega_M \geq 0$, the spectroscopically confirmed SNe Ia are statistically consistent with $q_0 < 0$ at the $2.8\sigma$ and $3.9\sigma$ confidence levels, and with $\Omega_\Lambda > 0$ at the $3.0\sigma$ and $4.0\sigma$ confidence levels, for two different fitting methods respectively. Fixing a "minimal" mass density, $\Omega_M = 0.2$, results in the weakest detection, $\Omega_\Lambda > 0$ at the $3.0\sigma$ confidence level from one of the two methods. For a flat-Universe prior ($\Omega_M + \Omega_\Lambda = 1$), the spectroscopically confirmed SNe Ia require $\Omega_\Lambda > 0$ at $7\sigma$ and $9\sigma$ formal significance for the two different fitting methods. A Universe closed by ordinary matter (i.e., $\Omega_M = 1$) is formally ruled out at the $7\sigma$ to $8\sigma$ confidence level for the two different fitting methods.

May 1998

# Dark Energy

High-z Supernova Search Team

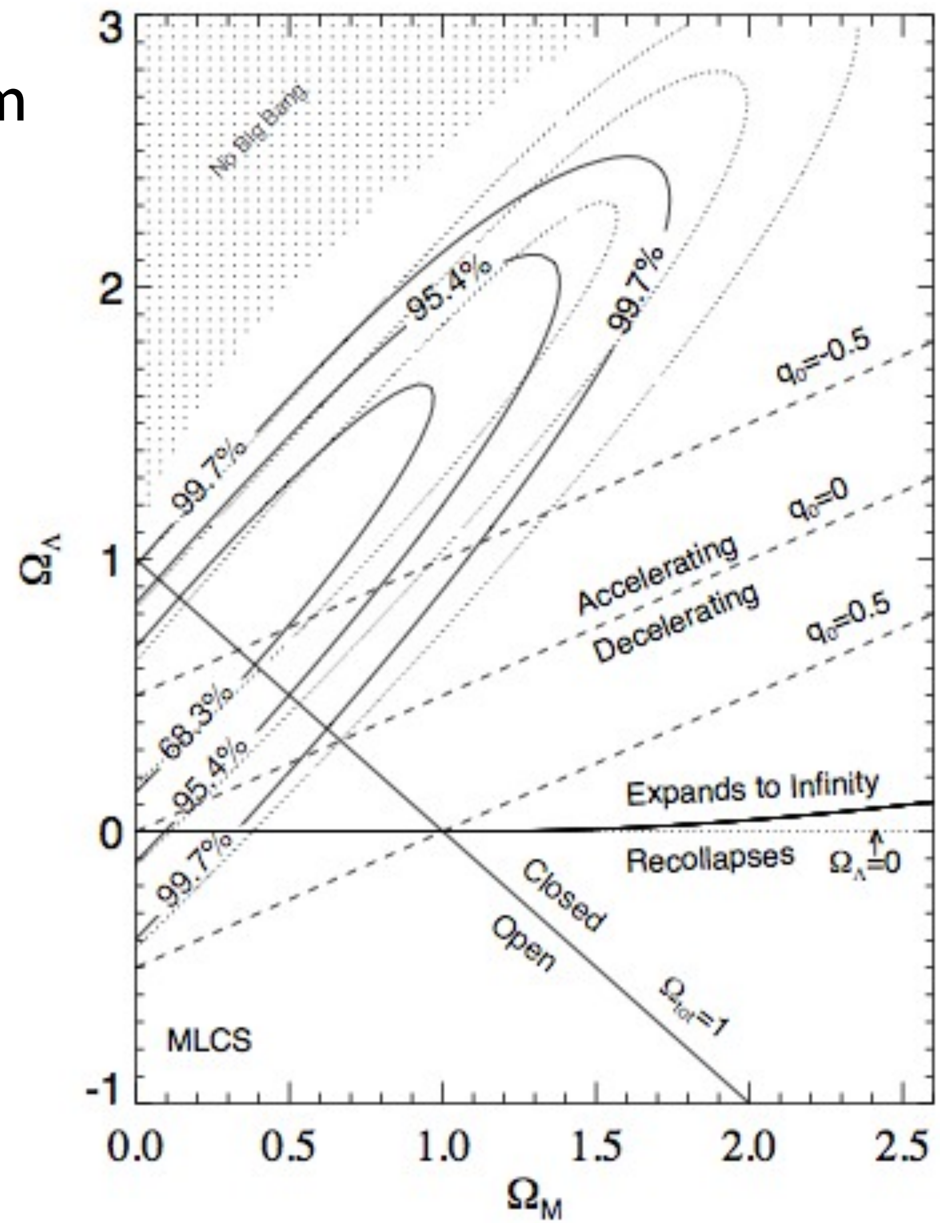

# Dark Energy

## MEASUREMENTS OF $\Omega$ AND $\Lambda$ FROM 42 HIGH-REDSHIFT SUPERNOVAE

S. PERLMUTTER[1], G. ALDERING, G. GOLDHABER[1], R.A. KNOP, P. NUGENT,
P. G. CASTRO[2], S. DEUSTUA, S. FABBRO[3], A. GOOBAR[4],
D. E. GROOM, I. M. HOOK[5], A. G. KIM[1,6], M. Y. KIM, J. C. LEE[7],
N. J. NUNES[2], R. PAIN[3], C. R. PENNYPACKER[8], R. QUIMBY
Institute for Nuclear and Particle Astrophysics,
E. O. Lawrence Berkeley National Laboratory, Berkeley, California 94720.
C. LIDMAN
European Southern Observatory, La Silla, Chile.
R. S. ELLIS, M. IRWIN, R. G. MCMAHON
Institute of Astronomy, Cambridge, United Kingdom.
P. RUIZ-LAPUENTE
Department of Astronomy, University of Barcelona, Barcelona, Spain.
N. WALTON
Isaac Newton Group, La Palma, Spain.
B. SCHAEFER
Department of Astronomy, Yale University, New Haven, Connecticut.
B. J. BOYLE
Anglo-Australian Observatory, Sydney, Australia.
A. V. FILIPPENKO, T. MATHESON
Department of Astronomy, University of California, Berkeley, CA.
A. S. FRUCHTER, N. PANAGIA[9]
Space Telescope Science Institute, Baltimore, Maryland.
H. J. M. NEWBERG
Fermi National Laboratory, Batavia, Illinois.
W. J. COUCH
University of New South Wales, Sydney, Australia.
(THE SUPERNOVA COSMOLOGY PROJECT)

December 1998

# Dark Energy

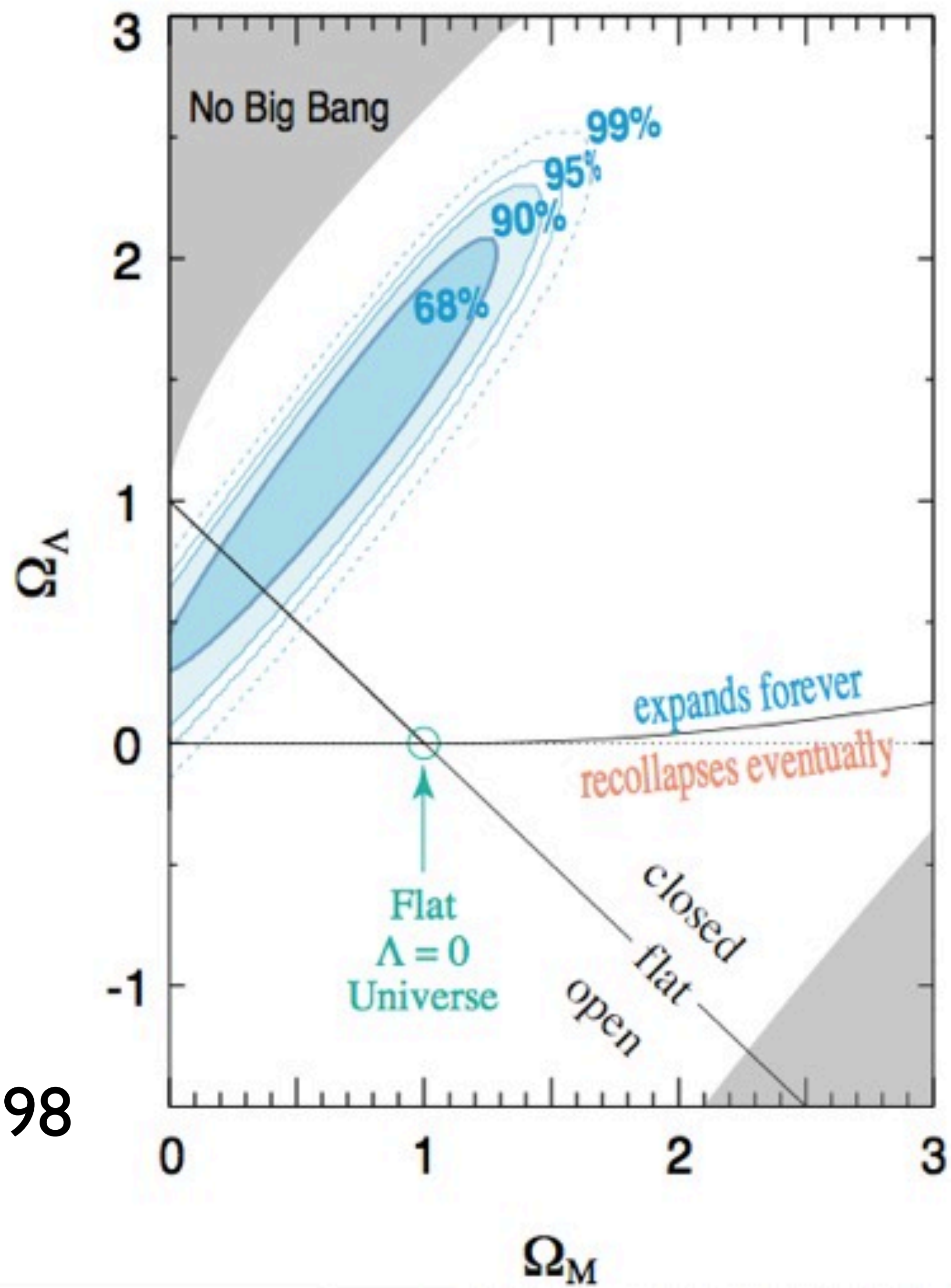


December 1998

# Dark Energy

Joint lightcurve analysis (JLA)

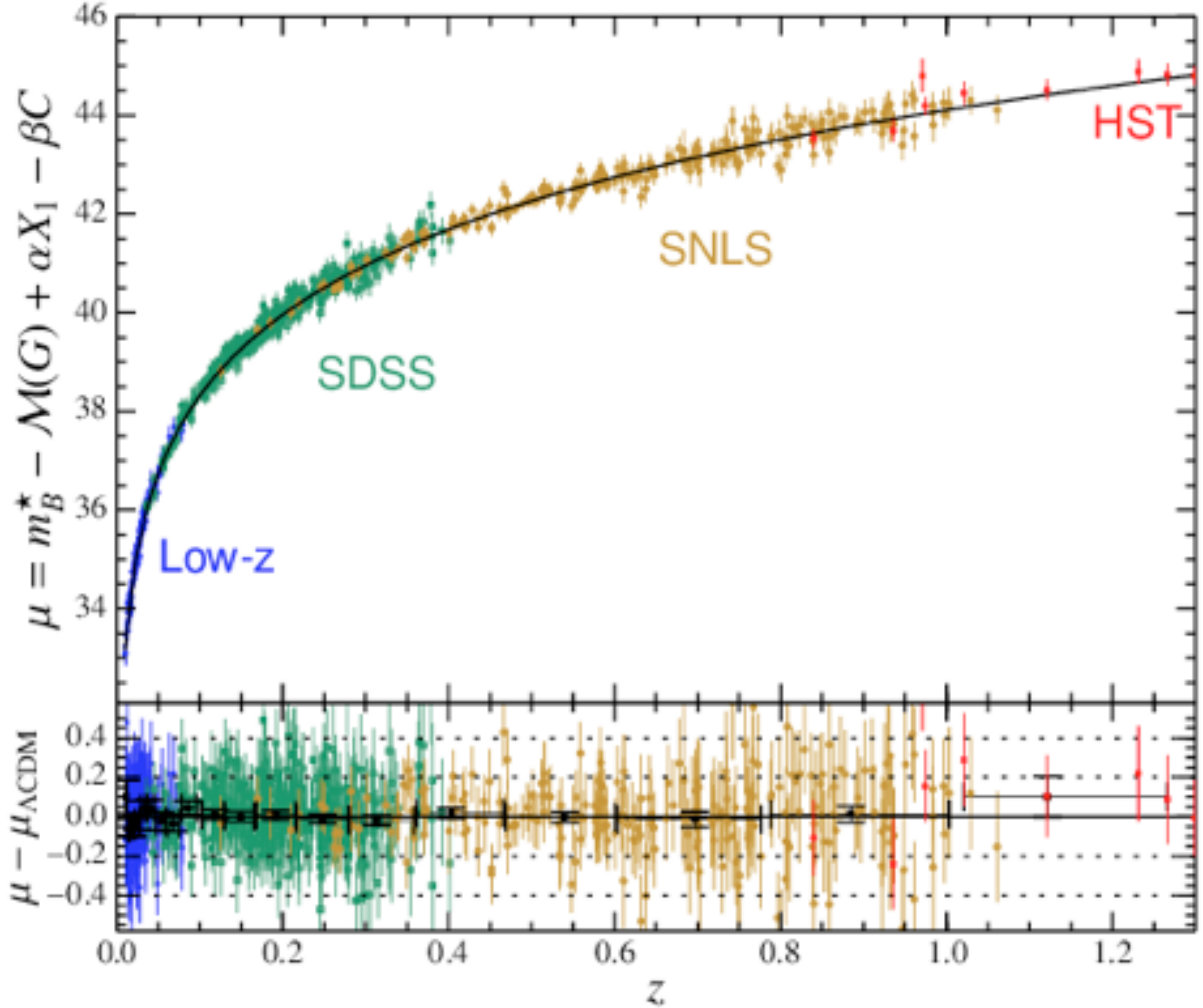

# Dark Energy

Joint lightcurve analysis (JLA)